EUENANTIORNITHINE BIRDS FROM THE LATE CRETACEOUS OF EL BRETE (ARGENTINA)

CYRIL A. WALKER and GARETH J. DYKE

(Received 26 August 2009, Accepted 11 January 2010)

Abstract

A taxonomic illustrated review of the Late Cretaceous fossil birds known from the Argentine locality of El Brete (Salta Province, Patagonia, Argentina) is presented here for the first time. Although some of these specimens were first reported in the early 1980s, and then a handful more were presented in literature thoughout the 1990s, this important collection of fossil birds has largely remained undescribed since it was gathered 30 years ago. This is in spite of the fact that the El Brete collection provided the basis of C.A. Walker's insight that enantiornithine birds are anatomically—and phylogenetically—distinct from all other living and extinct avians. A catalogue of the known specimens from this site is also presented, and many elements are illustrated for the first time. We revise the anatomy of taxa from El Brete and provide complete lists of referred specimens, based on casts of the collection held in the Natural History Museum, London, and Walker's original manuscript. Six valid euenantiornithine birds are currently known from the El Brete locality—*Enantiornis* Walker 1981, *Lectavis* Chiappe 1993, *Soroavisaurus* Chiappe 1993, *Yungavolucris* Chiappe 1993, and *Martinavis* Walker *et al.* 2007—alongside a new taxon described and documented in this paper (*Elbretornis*). This new fossil euenantiornithine is remarkable because its humerus is highly pneumatised, more extensively than any other known Mesozoic fossil bird. The physiological and evolutionary implications of this bird and the other El Brete taxa are discussed.

Introduction

Enantiornithine birds (Aves: Ornithothoraces: Enantiornithes) are now known to be the most diverse of the lineages of avians known from the Cretaceous. These birds are universally considered to be anatomically and functionally distinct from their modern neornithine counterparts (Fig. 1) and are known from sedimentary deposits on all continents around the world, with the exception of Antarctica (Fig. 2). Collection effort over the last twenty years has resulted in a steady increase in species of enantiornithine birds (Fountaine *et al.* 2005), but this was not always the case.

In the late 1970s, pre-cladistic views of avian phylogeny and classification recognised three 'subclasses' of birds, referred to as the 'Archaeornithes', 'Odontornithes' and 'Neornithes' (e.g., Brodkorb 1976; Walker 1981; Martin 1983). Examination of the morphology of the El Brete specimens, brought to London by J. Bonaparte, led Walker to name a new avian group—which he termed the subclass 'Enantiornithes' (Walker 1981; Walker *et al.* 2007)—to accommodate these (at the time) strange forms. Walker (1981) initially based this new 'subclass' on a selection of associated forelimb elements and a further assortment of other bones to show the variety within the collection. Although naming just one taxon (*Enantiornis*), it was clear to Walker (1981) that several closely related species of birds were represented in the El Brete collection. However, a comprehensive review of the known material was beyond the scope of his 1981 paper.

Irish Journal of Earth Sciences **27** (2009), 15–62
doi: 10.3318/IJES.2010.27.15

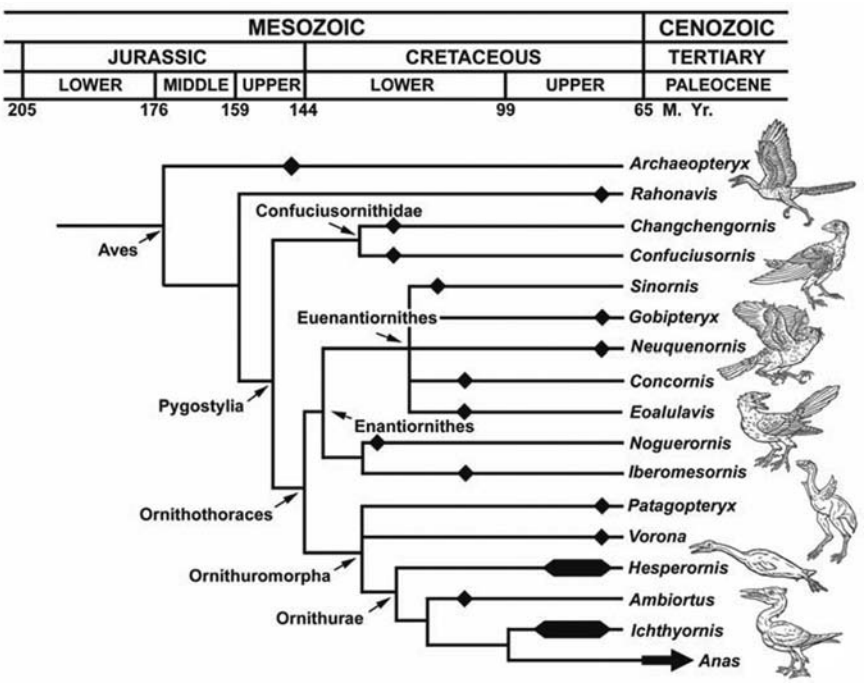

Fig. 1—Summary phylogenetic tree to show the current consensus with regard to relationships among Mesozoic birds (including Neornithes) (modified from Chiappe and Dyke 2002).

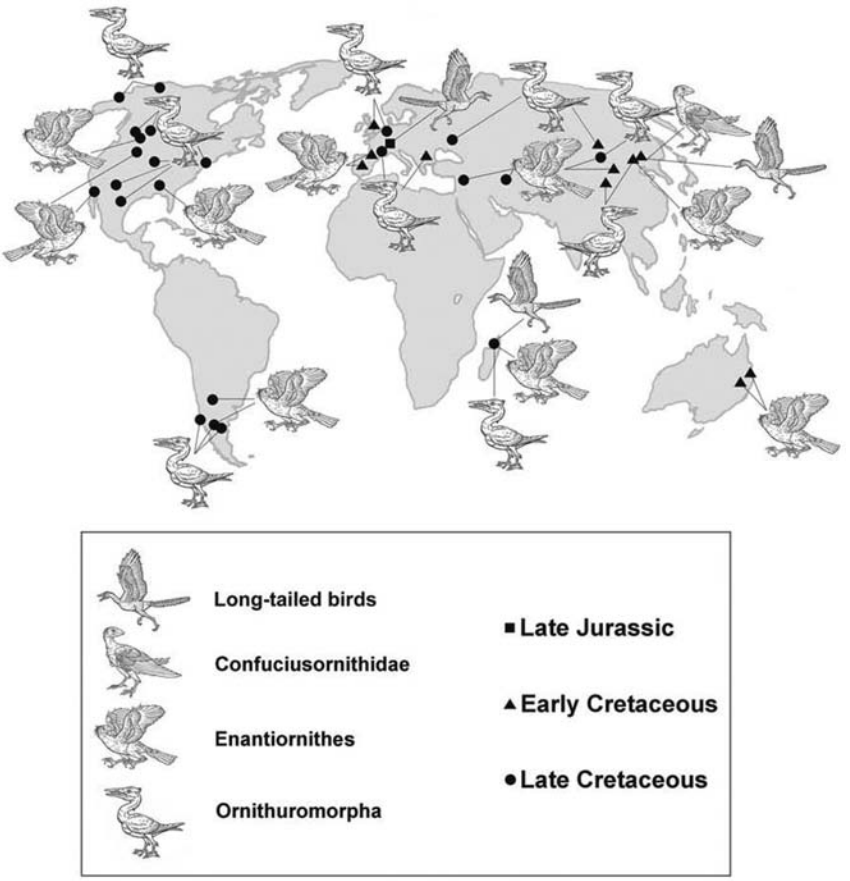

Fig. 2—Map to show our current understanding of the global distribution of enantiornithine, and other, birds (modified from Chiappe and Dyke 2002).

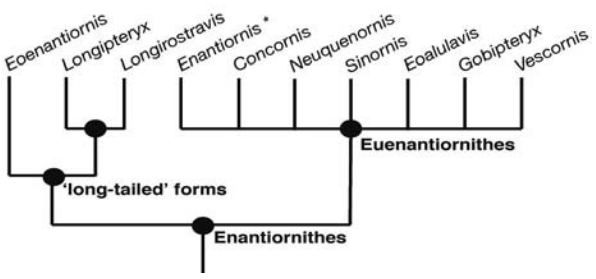

Fig. 3—Sketch of a phylogenetic tree intended to summarise current consensus regarding relationships amongst well-preserved Enantiornithes (modified from Chiappe and Walker 2002; Chiappe *et al.* 2007 and O'Connor *et al.* 2006). The asterisk denotes the hypothesised position of the El Brete euenantiornithine *Enantiornis leali* (see text for details); although currently untested by phylogenetic analysis the remainder of the El Brete taxa recognised in this paper are also placed within this taxonomic group.

Although heavily critiqued at the time (see the historical review in Walker *et al.* 2007), Walker's (1981) initial work provided the eventual impetus for an explosion in re-interpretations of already described species (e.g., Harrison and Walker 1973; Brodkorb 1976; Nessov 1984; Brett-Surman and Paul 1985), discoveries and analyses of Enantiornithes leading to our understanding of their current taxonomic and paleobiogeographic diversity (e.g., Martin 1983; Kurochkin 1995; Chiappe and Walker 2002; Fountaine *et al.* 2005; Chiappe 2007; Chiappe *et al.* 2007). To date more than 80 specimens representing more than 20 species of these birds have been described from all over the world (Fig. 2), comprising a very significant proportion of the known Mesozoic avifauna (Fountaine *et al.* 2005; Chiappe 2007). In addition to their taxonomic variability, we also know that these birds were highly diverse in their flight styles, wing and leg morphologies, at least to a similar extent as modern birds (Chiappe *et al.* 2007). Nevertheless, despite their anatomical distinctiveness and likely ecological variability, the evolutionary relationships between taxa of enantiornithines still remain poorly resolved and little understood (Fig. 3) (Chiappe and Walker 2002; Chiappe *et al.* 2007; J. O'Connor pers. comm. 2007).

In this paper, we add significantly to the known morphological variation of enantiornithines by reviewing all the taxa from the Late Cretaceous Argentine locality of El Brete (Fig. 4). The presence of birds at this site has been well-known since the late 1970s (Walker 1981; Chiappe and Walker 2002), but the bulk of specimens that were collected still await anatomical description and analysis. Thus we discuss the taxonomy of the few species previously described from this site (Walker 1981; Chiappe 1991, 1993; Chiappe and Walker 2002), and augment the existing anatomical description of the large euenantiornithine *Enantiornis leali* (Walker 1981; Chiappe 1996). We also add to the known fossil material of the recently described *Martinavis* (Walker *et al.* 2007) and describe the postcranial remains of another new and unique early avian (*Elbretornis*). As has been demonstrated previously (Walker *et al.* 2007), these southern hemisphere euenantiornithines share numerous anatomical similarities with taxa of the same age from the northern hemisphere, in particular those known from the late Cretaceous of Mexico (*Alexornis*; Brodkorb 1976), USA (Walker *et al.* 2007) and Europe (Buffetaut 1998; Walker *et al.* 2007; Ösi 2008; Dyke and Ösi 2010) (Fig. 2). The biogeographic implications of the distribution of Cretaceous euenantiornithines is further discussed in this paper, as are the unique

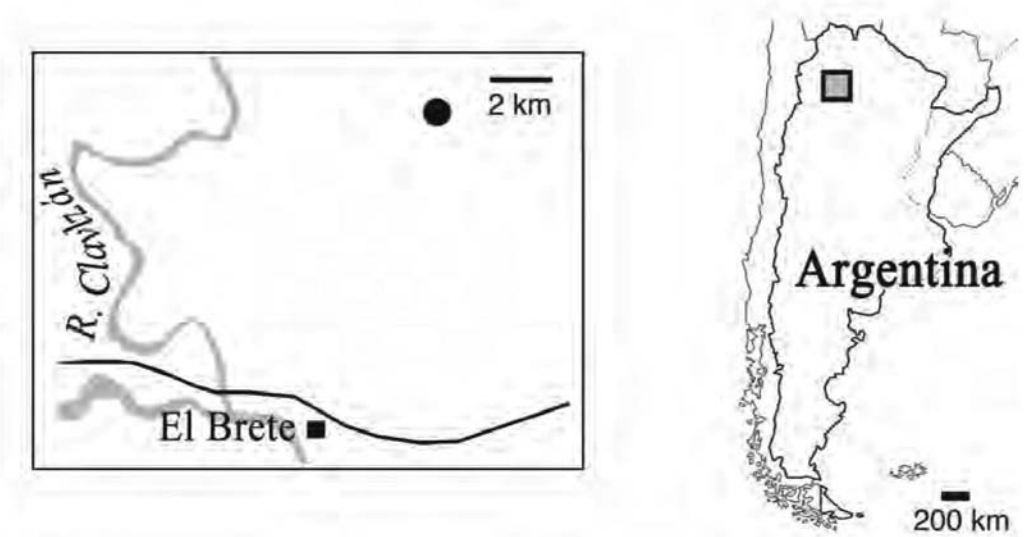

Fig. 4—Map to show the location of the Late Cretaceous El Brete site (inset) in Patagonia, southern Argentina (from Walker *et al.* 2007).

patterns of postcranial pneumatisation seen in these birds. Phylogenetic discussion of El Brete, and other euenantiornithines, must await the results of a large-scale cladistic analysis: the primary aim of this study is to present a review of the anatomical variability seen within the El Brete collection and to tidy up the taxonomy of this assemblage of fossil birds.

Materials and methods

Our understanding is that Argentine specimens examined for this study are the property of the Fundación-Instituto Miguel Lillo, Tucumán, Argentina (**PVL**), and were collected by J. Bonaparte and J. Leal between 1974 and 1976 (Walker 1981; Chiappe 1993; Walker *et al.* 2007) see Table 1 at the end of this paper. Casts of these specimens are held in the collections of the Department of Palaeontology, in the Natural History Museum, London, UK (**BMNH**); we have partly based our anatomical descriptions and conclusions on an unpublished manuscript written by C.A. Walker in the mid-1980s, and added information gleaned from these BMNH casts, as well as photographs and drawings of the fossils prepared for Walker's original unpublished manuscript. The entire El Brete collection was brought to London by J. Bonaparte in the late 1970s for appraisal, and study, by Walker (Walker *et al.* 2007; see also Chiappe 1991, 2007; J. Bonaparte, pers. comm. 2008); additional specimens referred to in this paper are held in the collections of the University of Kansas Museum of Natural History (**KU-NM**), and the Musée de Cruzy, Cruzy (l'Association Culturelle, Archéologique et Paléontologique de l'Ouest Biterrois), France (**ACAP**). For the most part, we use the standard English equivalents of avian anatomical nomenclature (i.e., statement of homology *sensu* Baumel and Witmer 1993) based on Howard (1929), retaining Latin terminology when referring to muscles and ligament attachments (see Abbreviations). Measurements of specimens are given in Table 2.

The geology and regional context of the El Brete locality in north-western Argentina (Estancia El Brete, Department of Candelaria, Province of Salta) (Fig. 4) has been outlined by Bonaparte and Powell (1980), and Chiappe (1993). Sediments at this site are continental in origin and correspond to the Lecho Formation (Bonaparte and Powell 1980; Chiappe 1993), one of the units included in the Salta Group that in turn ranges from Lower Cretaceous to Lower Eocene in age. The age of the El Brete deposits themselves is undoubtedly Upper Cretaceous, but their exact correlation is uncertain; Bonaparte and Powell (1980) state that they are probably Maastrichtian. These sediments fill the so-called Andean Basin of north-western Argentina that extends west to northern Chile and north through most of Bolivia and southern Peru.

The bulk of the bird fossil material discussed in this paper was field collected as isolated elements (Walker 1981; Chiappe 2007; Walker *et al.* 2007). Bearing this in mind, museum numbers allocated to individual elements do not necessarily imply association (J. Bonaparte, pers. comm. 1980); however, enough corresponding bones do exist within the collection for some isolated elements to be assigned to the same taxa. What cannot be concluded, however, is a clear association *between* the forelimb and hindlimb elements known from this site. This lack of definitive specimen association presumably led Chiappe (1991, 1993) to erect El Brete taxa using bones from the hindlimb, the opposite approach to Walker (1981) who based his description of *Enantiornis* on forelimb anatomy. As we show in this paper, the latter approach is preferable because more definitive associations exist between bones of the forelimb and shoulder girdle than are evident between elements of the more 'spectacular' looking hindlimbs (Table 1).

Abbreviations

The following anatomical abbreviations are used in the figures: ac—acetabulum; am—angulus medialis (internal distal angle); api—anterior ilium; arl—attachment for 'round' ligament (fovea lig. capitis); at—antitrochanter; ba—bicipital attachment (facies articularis bicipitalis); bf—brachial fossa (fossa brachialis); bs—brachial surface (facies bicipitalis); ca—coracoidal articulation (tuberculum coracoideum); cg—capital groove (incisura capitis); chs—coracohumeral surface (impressio lig. acrocoracohumeralis); dc—deltopectoral crest (crista); df—dorsal foramen (coracoid); dfo—dorsal fossa (impressio m. sternocoracoidei); dpn—depression; ec—external cotyla (cotyla dorsalis); ecp—ectepicondyle (epicondylus dorsalis); elp—external ligamental prominence; ent—entepicondyle (epicondylus ventralis); entp—entepicondylar prominence; ep—extensor process (processus extensorius); exc—external condyle (condylus lateralis); ext—external tuberosity (tuberculum dorsale); fa—furcular articulation (facies articularis clavicularis); fmb—facies articularis radialis; gf—glenoid facet (facies articularis humeralis); gr—groove; gt—greater trochanter (trochanter femoris); hd—head (caput humeri, caput femori); hyp—hypapophysis; iif—ilio-ischiadic fenestra; il—illium; ilf—iliac facet (impressiones iliotrochanteris); ic—intercotyla crest; is—ischium; inc—internal condyle (condylus ventralis); it—internal tuberosity (tuberculum

ventrale); lf—lateral face (of capital groove); lt—lesser trochanter (iliotrochanter); ns—neural spine; o—olecranon; occ—outer cnemial crest (crista cnemalis lateralis); of—olecranon fossa (fossa olecrani); p—pubic penduncle; pa—popliteal area (fossa poplitea); pf, pfn—pneumatic fossa (crus fossa); pl—processus lateralis (sterno-coracoidal process); plc—pleurocoel; po—pollex (alula); pof—polical facet (processus alularis); ppi—posterior ilium; prz—prezygapophysis; ptz—postzygapophysis; sa—sulcus articularis (sulcus m. supracoracoidei); scf—scapula facet (cotyla scapularis); scv—synsacral caudal vertebrae; ts—transverse surface.

Systematic palaeontology

Aves Linnaeus, 1758
Ornithothoraces Chiappe, 1996
Enantiornithes Walker, 1981
Euenantiornithes Chiappe, 2002

Definition and diagnosis

Both node- and character-based diagnoses for Euenantiornithes were provided by Chiappe and Walker (2002) and Chiappe *et al.* (2007). Since publication of the phylogenetic studies of Chiappe (2002) and Chiappe and Walker (2002), the only other work to deal specifically with the relationships of these birds is Chiappe *et al.* (2007). Although the monophyly of Enantiornithes, and its nested clade Euenantiornithes, has not seriously been questioned,

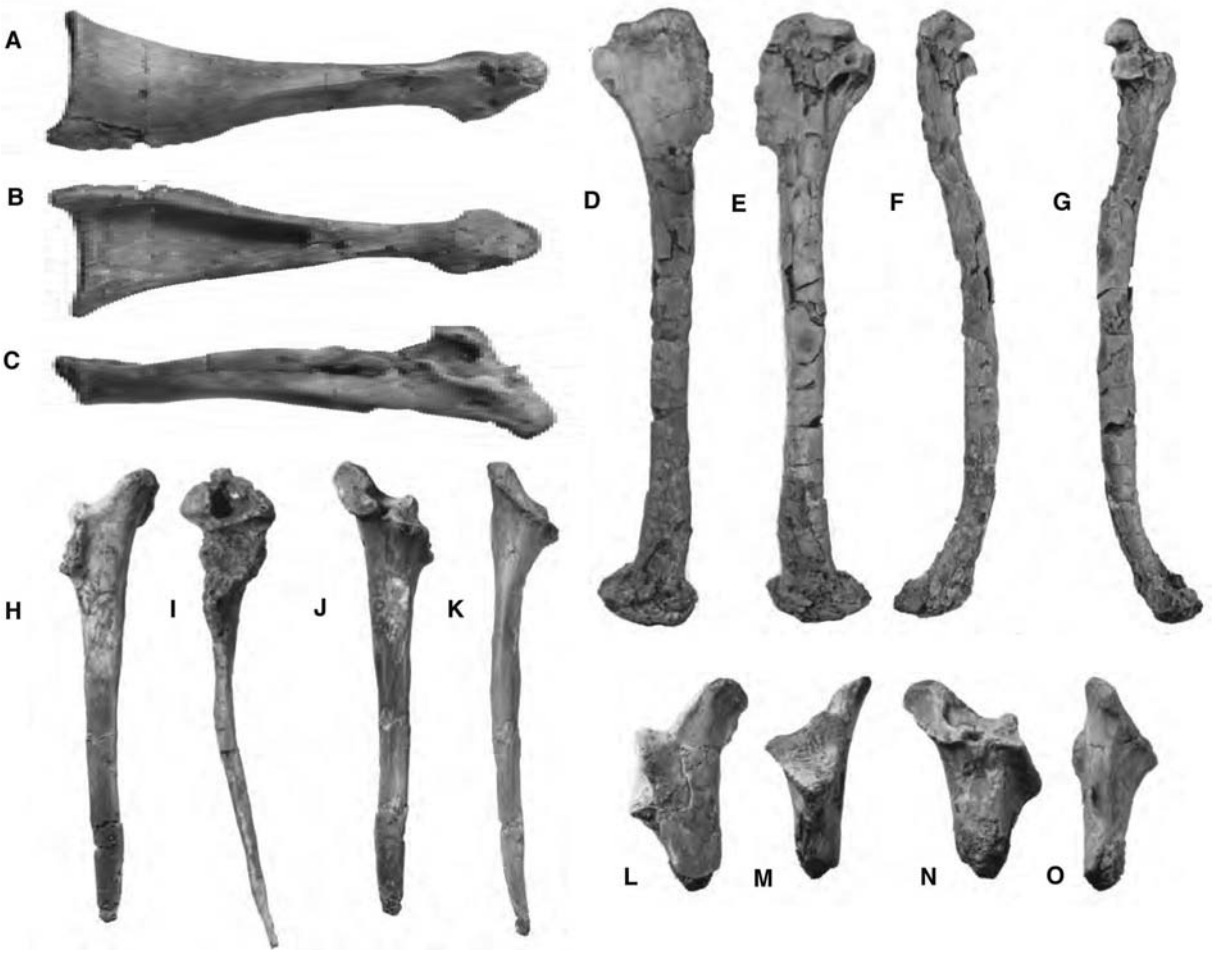

Fig. 5—Photographs of fossil bones referred to *Enantiornis leali* Walker: holotype left coracoid (PVL 4035) in ventral (**A**), dorsal (**B**) and medial (**C**) views; referred left humerus (PVL 4020) in cranial (**D**), caudal (**E**) and lateral (**F, G**) views; referred left scapula (PVL 4039) in lateral (**H**), ventral (**I**), medial (**J**) and dorsal (**K**) views; holotype left scapula (PVL 4035) in lateral (**L**), ventral (**M**), medial (**N**) and dorsal (**O**) views. For measurements see Table 2.

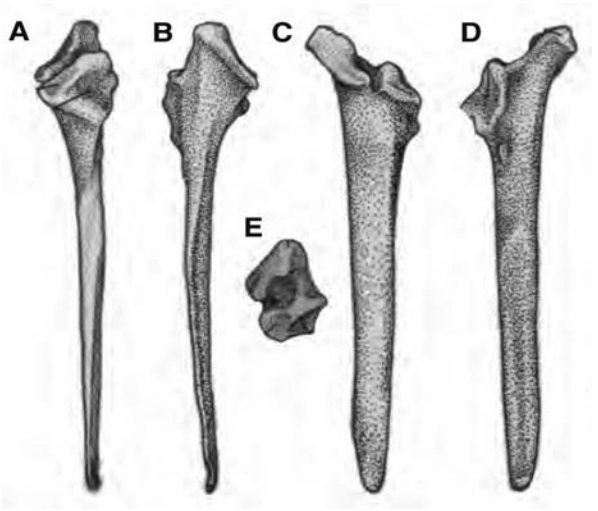

Fig. 6—*Enantiornis leali*, drawings of referred left scapula (PVL 4039) in ventral (**A**), dorsal (**B**), medial (**C**), lateral (**D**) and proximal (**E**) views. For measurements see Table 2.

little phylogenetic resolution has so far been achieved between included taxa. Even larger-scale analysis of a much expanded dataset has failed to clearly elucidate patterns of relationship amongst the more than twenty valid enantiornithine taxa (Fig. 3) (J. O'Connor, pers. comm. 2007).

Enantiornis Walker 1981
Figures 5–12, 14–16; Table 2

Emended diagnosis
This taxon was originally diagnosed by Walker (1981), and was modified and emphasised by Chiappe (1996) (see also Chiappe 2002; Chiappe and Walker 2002). These birds are characterised by the presence of a large perforating, pneumatic foramen on the distal end of the ulna (Figs 8H, 12A). Additional apomorphic features (Walker 1981; Chiappe 1996; Chiappe and Walker 2002; Chiappe *et al.* 2007) include: a scapula with a distinct depression in the acromion process (anterior to the coracoid articulation), and the presence of a narrow notch just ventral to it (Fig. 6); a coracoid with a fenestra in the medial wall of the neck (Figs 7, 10); a humerus with a narrow pneumatic fossa, sometimes perforated by a canal running proximodistally through the internal tuberosity; a bicipital crest markedly projected cranially; an external tuberosity that rises above the level of the head in caudal view (Fig. 11); the medial edge of the internal condyle of the ulna straight; and a large pit present in ventral view above the distal articulation of the ulna (this contains the large foramen) (Fig. 12A–C).

Enantiornis leali Walker 1981 (Chiappe 1996)
Figures 5–13; Table 2

Holotype
PVL 4035, cranial end of a left scapula (Fig. 5L–O; Fig. 8B), complete left coracoid (Fig. 5A–C; Fig. 7A–F; Fig. 8C), and the proximal portion of a left humerus (Fig. 8A; Fig. 11). Because these bones were only supposedly collected in association (J. Bonaparte, pers. comm. 1980; Walker 1981; Chiappe 1996, 2007), it is not completely certain that PVL 4035 pertains to a single individual. As a result, it may be necessary in the future to designate a lectotype element from these three bones (PVL 4035).

Referred specimens
PVL 4020, imperfect left scapula and coracoid (Fig. 10), complete but poorly preserved left humerus (Fig. 5D–G), imperfect left ulna (Fig. 12A–C), proximal portions of the right ulna and radius (Fig. 8G–L), right scapholunar, right cuneiform and distally imperfect right carpometacarpus with pollex (although this pollex is unfortunately lost) (Fig. 9; Fig. 13). These bones were definitely collected in association, indeed they were originally cemented together by a matrix in articulation (the final preparation of PVL 4020 was undertaken by staff at KU-NM) . PVL 4039 (Fig. 5H–K; Fig. 6), PVL 4055 (two complete scapulae) and PVL 4029 (the caudal portion of a right coracoid) were subsequently referred to *Enantiornis leali* based on comparisons and size (Chiappe 1996) (Table 1).

Tentatively referred specimens
PVL 4023, proximal end of a right ulna (Fig. 12D–G); PVL 4043, proximal end of a left humerus (Fig. 8A).

Diagnosis
As for genus, only currently recognised species.

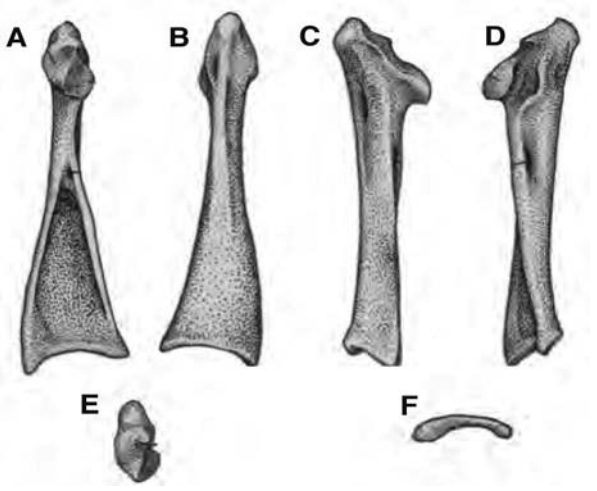

Fig. 7—*Enantiornis leali*, drawings of the holotype coracoid (PVL 4035) in dorsal (**A**), ventral (**B**), lateral (**C**), medial (**D**), proximal (**E**) and sternal (**F**) views. For measurements see Table 2.

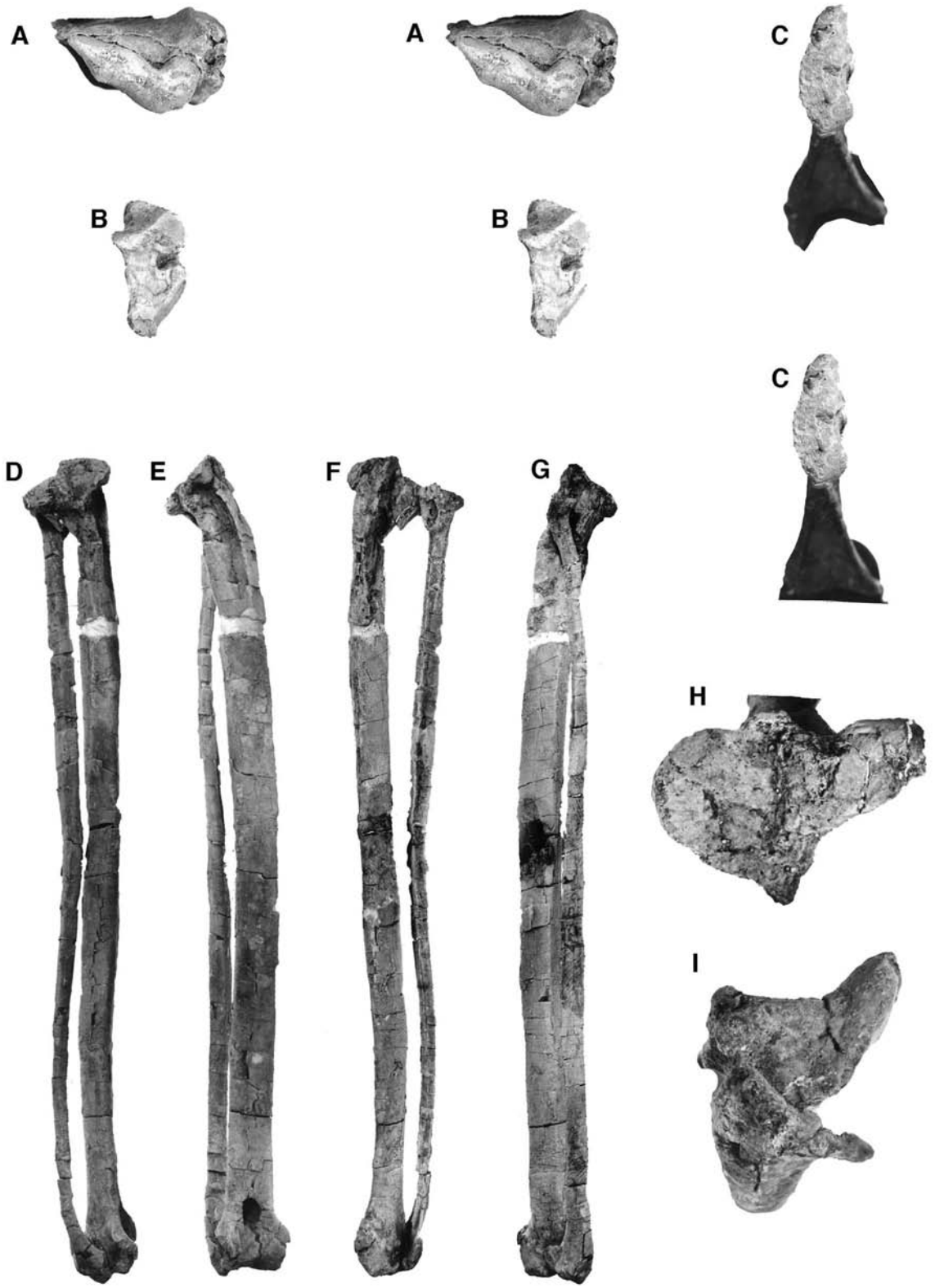

Fig. 8—Photographs of fossil bones referred to *Enantiornis leali*: holotype proximal left humerus (PVL 4035), (**A**); holotype proximal left scapula (PVL 4035), stereo pairs (**B**); holotype proximal left coracoid (PVL 4035), stereo pairs (**C**); referred right ulna and radius (PVL 4020) in ventral (**D**), lateral (**E**), dorsal (**F**), lateral (**G**), proximal (**H**) and distal (**I**) views. For measurements see Table 2.

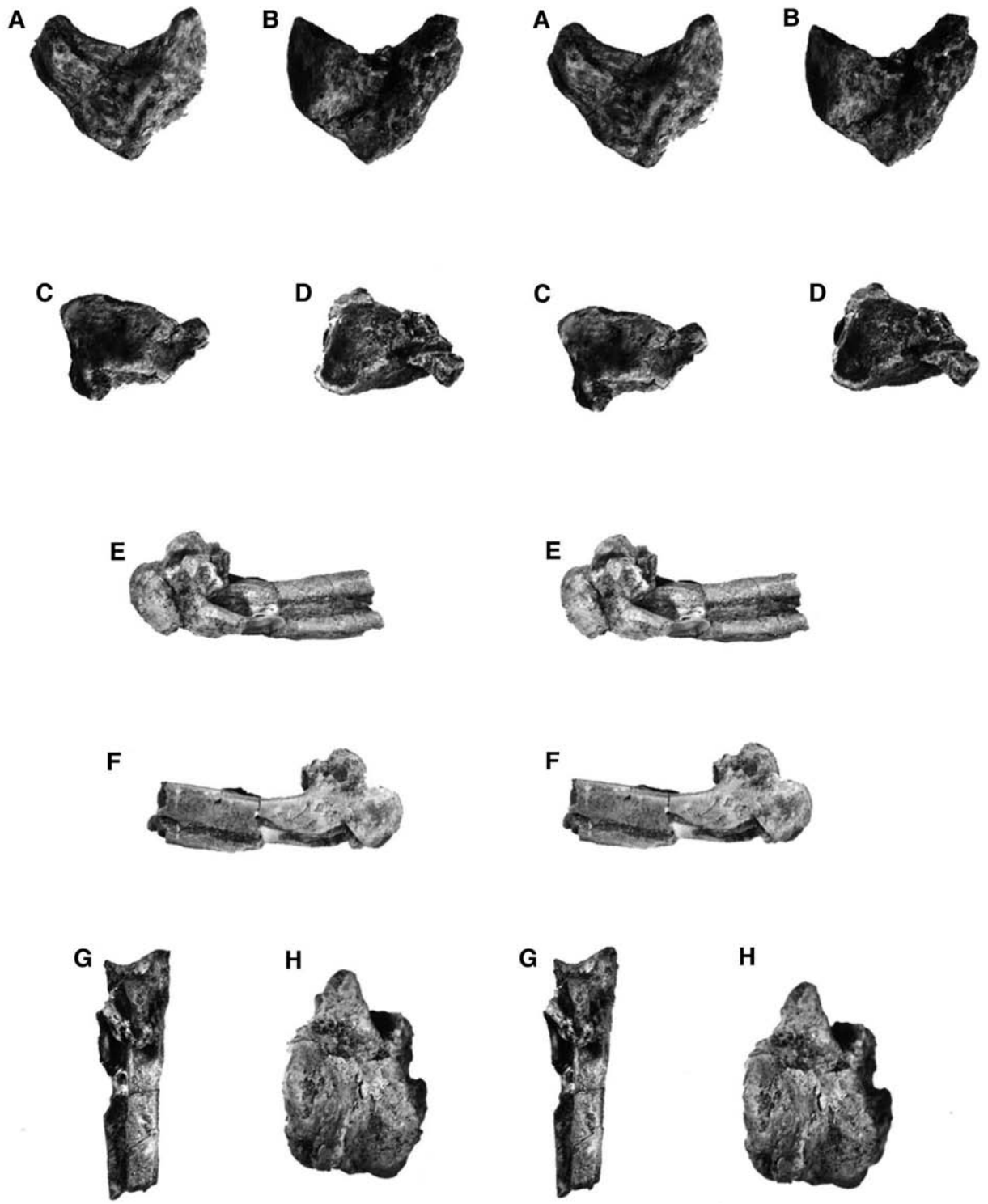

Fig. 9—Stereo photographs of associated wing elements referred to *Enantiornis leali* (PVL 4020): scapholunar (**A–B**); cuneiform (**C–D**); right carpometacarpus in dorsal (**E**), ventral (**F**), cranial (**G**) and proximal (**H**) views. For measurements see Table 2.

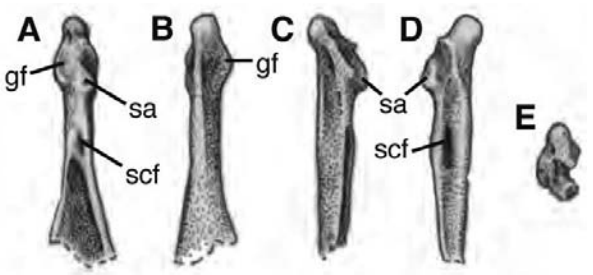

Fig. 10—*Enantiornis leali*, drawings of referred coracoid (PVL 4020) in dorsal (**A**), ventral (**B**), lateral (**C–D**) and cranial (**E**) views. This specimen is part of an associated series of bones and will aid future reconstruction of the *E. leali* forelimb skeleton. For measurements see Table 2

Description and comments

Brief descriptions of the forelimb anatomy of this taxon were provided in tabular form by Walker (1981). The humeral morphology of *E. leali* was subsequently described in more detail by Chiappe (1996) and the remaining known elements attributable to the thoracic girdle and sternum were discussed and described by Chiappe and Walker (2002). Additional bones from the

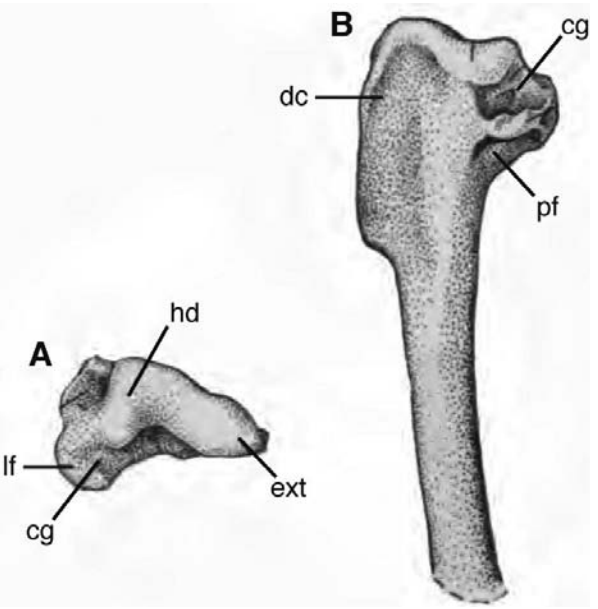

Fig. 11—*Enantiornis leali*, drawings of the holotype proximal left humerus (PVL 4035) in proximal (**A**) and caudal (**B**) views. For measurements see Table 2.

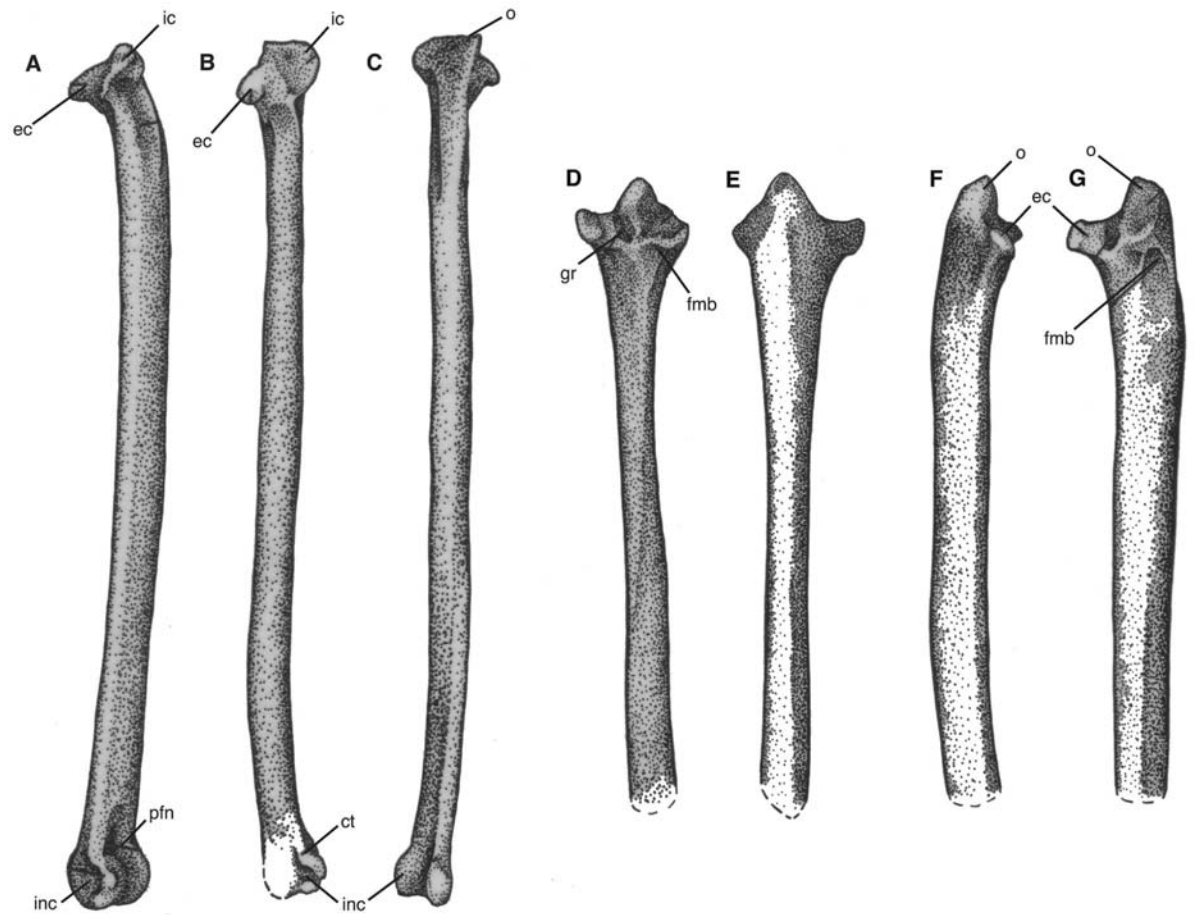

Fig. 12—*Enantiornis leali*, drawings of referred left ulna (PVL 4020) in dorsal (**A**), ventral, (**B**) and lateral (**C**) views; drawings of referred proximal right ulna (PVL 4023) in lateral (**D**), medial (**E**), dorsal (**F**) and ventral (**G**) views. For measurements see Table 2.

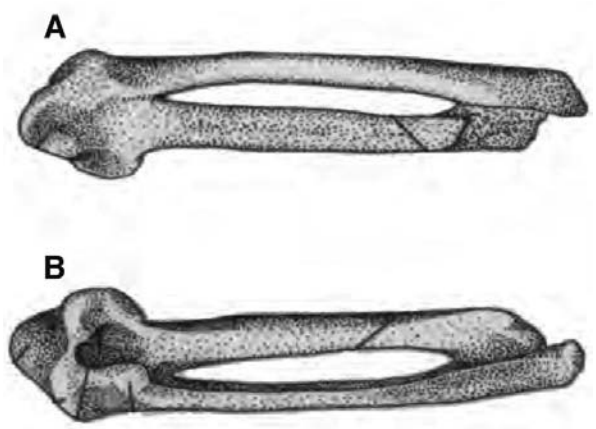

Fig. 13—*Enantiornis leali*, drawing of distally imperfect right carpometacarpus with pollex (PVL 4020). For measurements see Table 2.

original El Brete collection are referred here on the basis of their overlapping morphology with the holotype and referred specimens.

The isolated ulna (PVL 4023; Fig. 12D–G) is somewhat larger than corresponding bones certainly referrable to *E. leali*. Differences which are not the result of distortion during fossilisation are limited to the medial edge of the internal cotyla (which is not rounded as in PVL 4020) (cf. Figs 8 and 12). Additional structural differences between this bone and PVL 4020 are likely to have resulted from crushing. PVL 4023 (Fig. 12D–G) is nevertheless interesting because it is uncrushed and clearly shows the depressions for the facies m. brachialis and facies articularis radioulnaris proximalis, placed in the same positions as in neornithine birds.

In addition, although the proximal part of the humerus (PVL 4043) (Fig. 8A) is also slightly larger than corresponding bones previously referred to *E. leali*, it is similar in overall structure to the holotype and referred specimens (see Figs 7–9). Minor differences can be seen, however, in the shape of the proximal end: this surface in PVL 4043 is somewhat more robust with a more proximodistally inclined capital groove. The lateral edge of the deltoid crest is also proximally thick and the bicipital crest is more elongate. Furthermore, the head is approximately at the same level as the external tuberosity and does not overhang the capital groove. On the cranial surface, the scar situated between the deltoid crest and the depression distal to the head extends below the bicipital crest. The angle between the head and the bicipital surface is also less marked and the canal that perforates the internal tuberosity is either absent, or undiscovered. While this single specimen (PVL 4043) does appear to suggest the presence of an additional taxon anatomically distinct from *E. leali*, we refrain from erecting a new species until more fossil material becomes available.

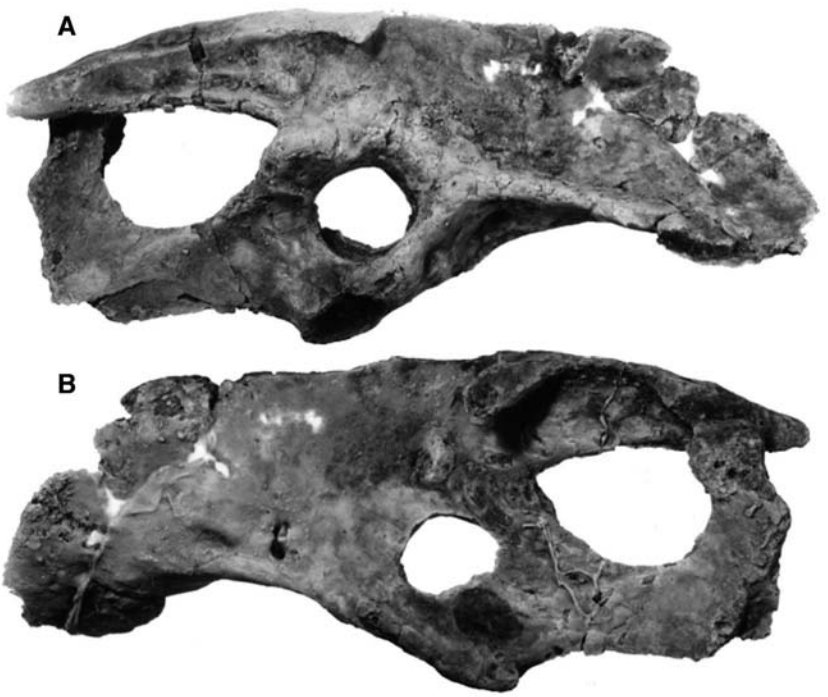

Fig. 14—Photographs of right ilium and ischium (PVL 4042) referred to *Enantiornis* sp. in lateral (**A**) and medial (**B**) views. For measurements see Table 2.

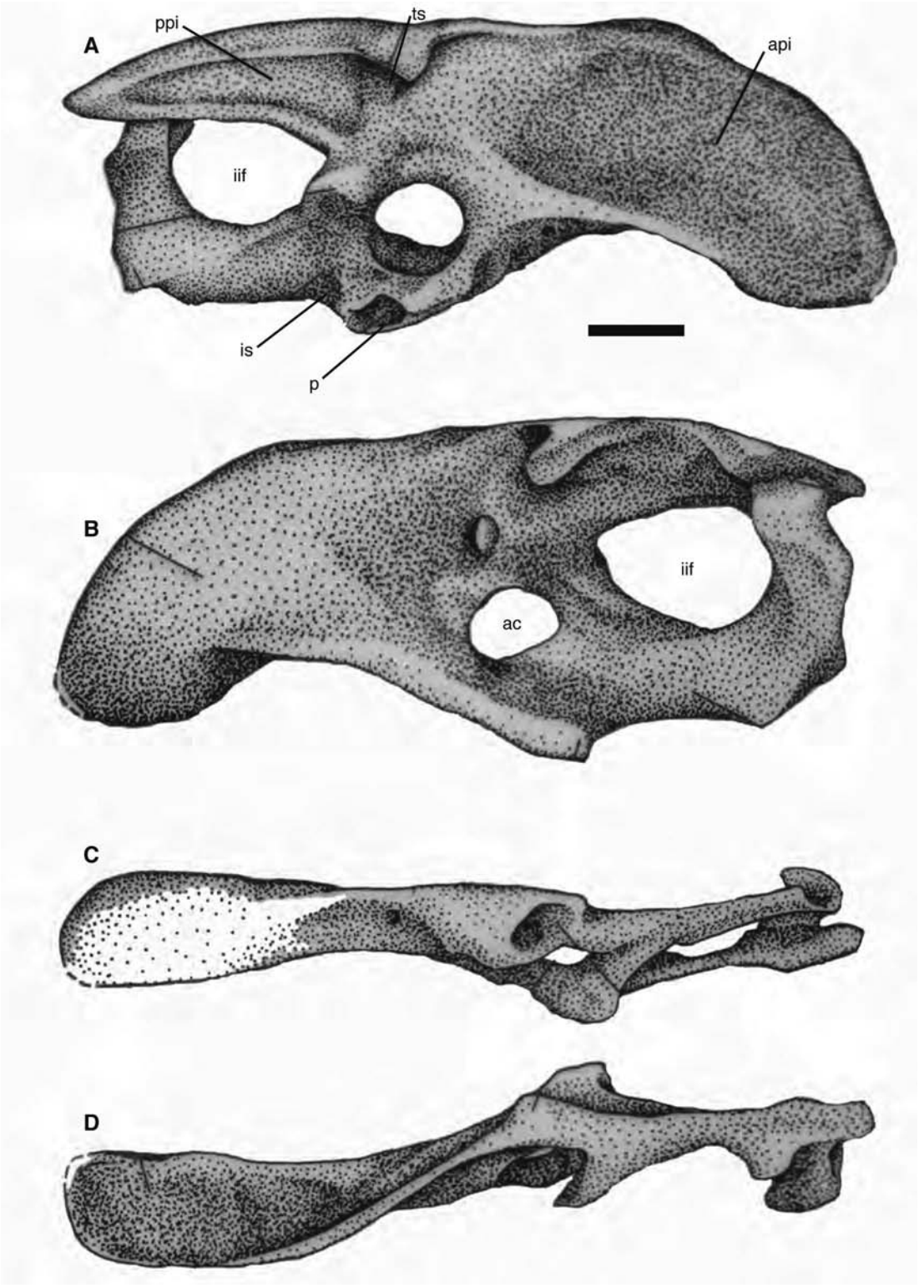

Fig. 15—Drawings of right ilium and ischium (PVL 4042) referred to *Enantiornis* sp. in lateral (**A**), medial (**B**), ventral (**C**) and dorsal (**D**) views. Scale-bar equals 10mm.

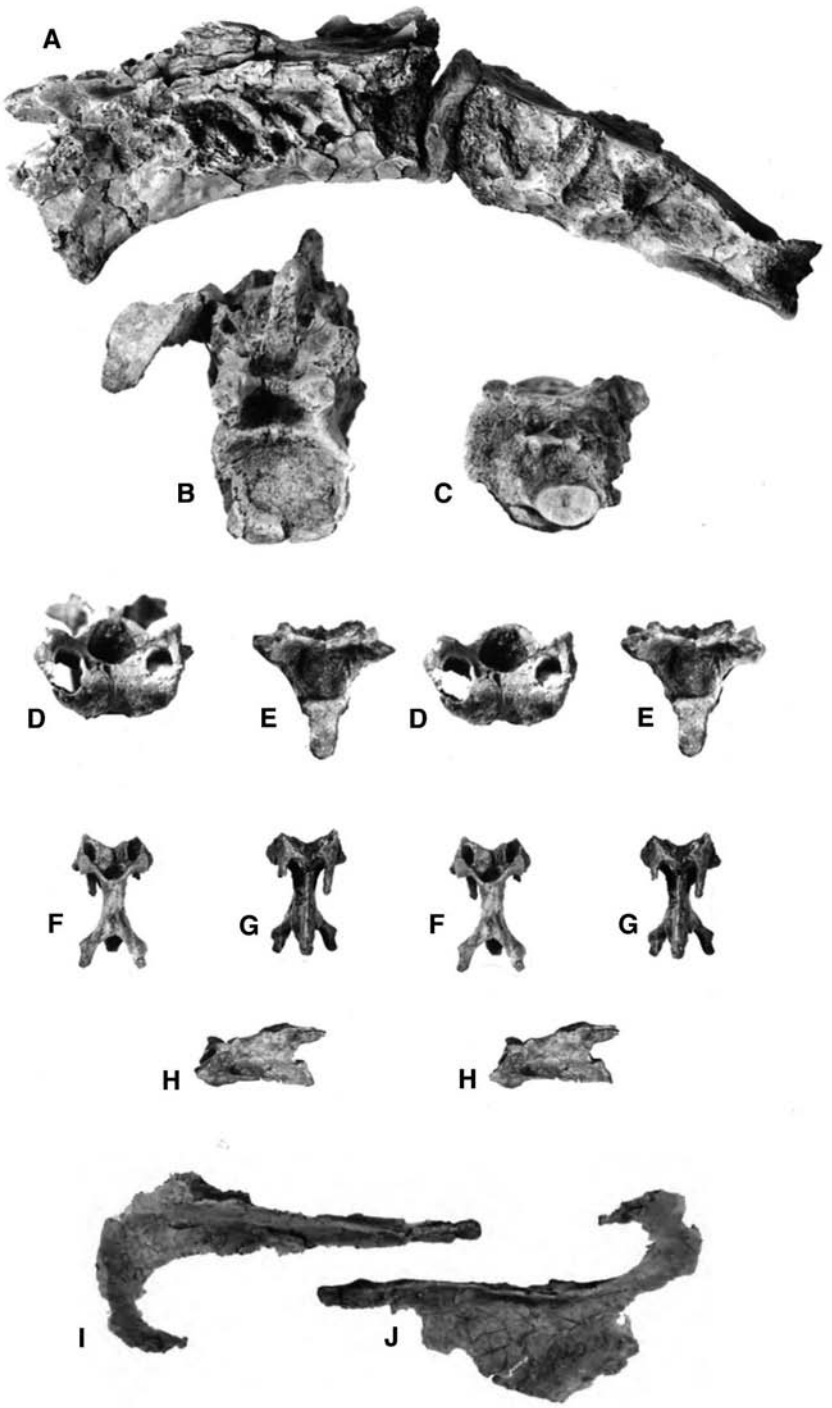

Fig. 16—Photographs of sacrum (PVL 4045) referred to *Enantiornis* sp. from left side (**A**) and in anterior (**B**) and posterior (**C**) views; stereo photographs of cervical vertebrae (PVL 4050) referred to *Enantiornis* sp. in anterior (**D**), posterior (**E**), dorsal (**F**), ventral (**G**) and left lateral (**H**) views; incomplete sternal plate with keel (PVL 4021) referred to *Enantiornis* sp. in ventral (**I**) and lateral (**J**) views. For measurements see Table 2.

Enantiornis sp.
Figures 14–16; Table 2

Referred specimens
An ilium and ischium (PVL 4042; Figs 14 and 15A–D), a poorly preserved sacrum (PVL 4045; Fig. 16A–C), two cervical vertebrae (PVL 4050 and PVL 4057; Fig. 16D–H), parts of metatarsals III and IV (PVL 4058), and an imperfect sternal plate with carinal keel (PVL 4021; Fig. 16I–J). Note that although the sternum (PVL 4021) bears the same number as a tibiotarsus and tarsometatarsus described by Chiappe (1993) as the holotype of *Lectavis bretincola* (Table 1), there is no apparent evidence (other than size) supporting association with these leg bones (J. Bonaparte, pers. comm. 1980). Consequently, this partial sternum needs to be allocated with a new number.

Description and comments
The two cervical vertebrae (PVL 4050 and 4057; Fig. 16D–H) are similar in morphology to those of extant neornithine birds in that they are excavated by pneumatic foramina on their lateral faces (Chiappe and Walker 2002), have elongate centra, well-developed diapophyses and long, caudally projecting cervical ribs (Fig. 16D–H). Because the centrum of PVL 4057 is shorter than its counterpart (PVL 4050), it is likely that this vertebra was positioned more anteriorly within the cervical series. PVL 4050 is likely to be cervical five or six; the two do not articulate with one another.

The ilium (PVL 4042; Figs 14 and 15) is similar in its morphology to this element in the basalmost avian *Archaeopteryx* (Chiappe and Witmer 2002; Mayr *et al.* 2005, 2006) although there are clear differences including that the anterior blade is short and deeply concave and the posterior projection is 'prong-like'

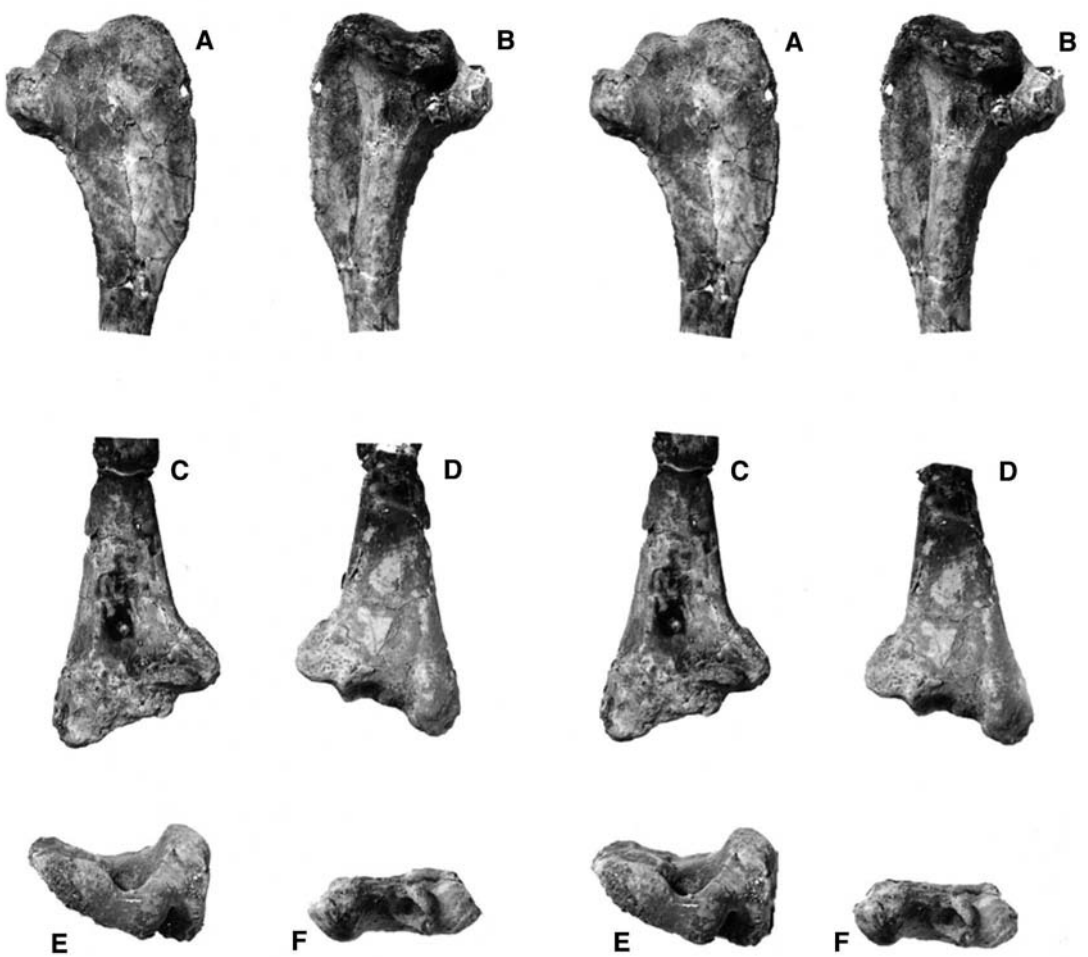

Fig. 17—Stereo photographs of the holotype specimen of *Martinavis vincei* (PVL 4054), left humerus in cranial (**A, C**), caudal (**B, D**), proximal (**E**) and distal (**F**) views. For measurements see Table 2.

(Fig. 15). An antitrochanter is present and is prominent with its dorsal edge deflected distinctly medially; there is also a well-developed supracetabular tubercle present above the acetabulum. However, because little of the pubis remains, it is unclear whether, or not, this element formed any part of the acetabular border; from the shape of the broken surface and the angle of the bone just below the acetabulum, it is likely that the pubis was projected caudally as in modern birds (Chiappe and Walker 2002). The ischium also resembles *Archaeopteryx* in that a projection rises up from the dorsal surface towards the ilium (Fig. 15); in PVL 4042, this projection reaches the posterior blade of ilium and produces the large ilioischiadic fenestra as seen in many extant birds. In earlier diverging fossil taxa (*Archaeopteryx*), the corresponding fenestra is very small and there is some doubt as to whether this upward projection actually reaches the iliac blade (Chiappe and Walker 2002).

The partial sternum (PVL 4021; Fig. 16I–J) is quite badly damaged, such that the cranial articulations for the coracoids have been lost and the ventral keel is worn away. The sternal plate is deeply notched, reminiscent of the condition seen in some living birds with limited powers of flight (e.g., Galliformes, Gruiformes).

Martinavis Walker, Buffetaut and Dyke 2007
Figures 17–33; Table 2

Diagnosis

As described by Walker *et al.* (2007), *Martinavis* is a euenantiornithine bird that possesses the following apomorphies of its humerus—based on the phylogenetic analyses detailed by Chiappe (2002), Chiappe and Walker (2002) and Chiappe *et al.* (2007): dorsal margin of humerus concave in its central portion, rising both ventrally and dorsally on either side; bicipital crest prominent (well-developed and broad); and ventral surface of bicipital crest bearing a small fossa for muscle attachment. In addition, this taxon shares with other members of Enantiornithes the presence of: an 'L-shaped' articulation between the proximal part of the humerus and the coracoid (seen in proximal view; Walker 1981); a well-marked depression underneath the proximal head of the humerus; weakly developed distal condyles; and a flat distal end that is not deflected

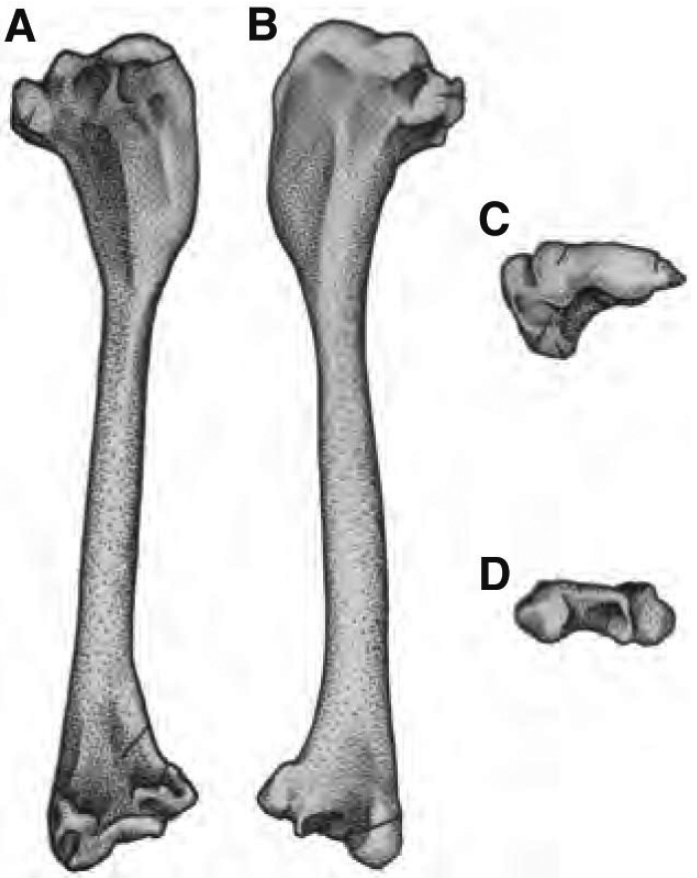

Fig. 18—Drawings of the holotype specimen of *Martinavis vincei* (PVL 4054), left humerus in cranial (**A**), caudal (**B**), proximal (**C**) and distal (**D**) views. For measurements see Table 2

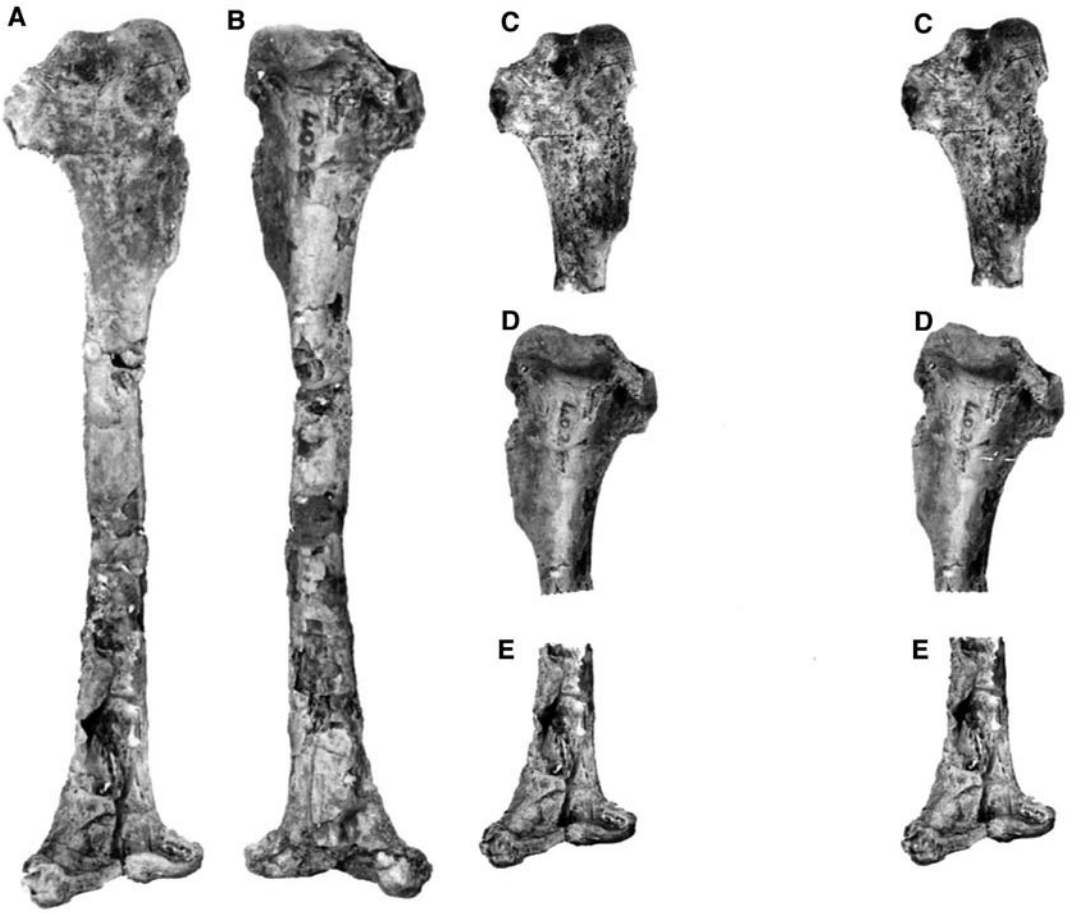

Fig.19—Photographs of the holotype specimen of *Martinavis saltariensis* (PVL 4025), left humerus in cranial (**A**), caudal (**B**), proximal cranial (**C**), proximal (**D**) and distal (**E**) views (**C–E** are stereo pairs). For measurements see Table 2.

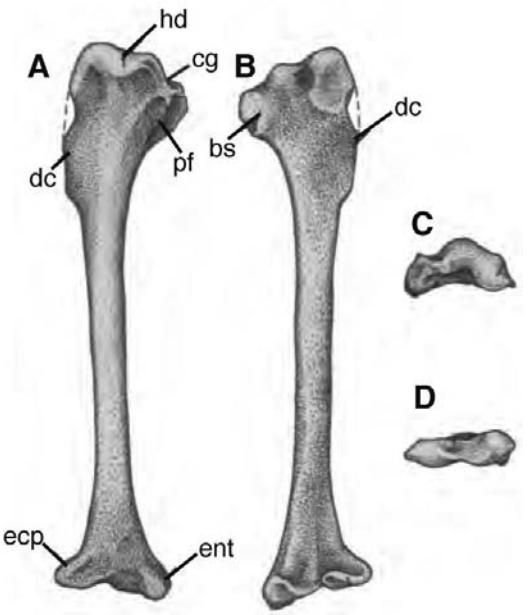

Fig. 20—Drawings of the holotype specimen of *Martinavis saltariensis* (PVL 4025), left humerus, in caudal (**A**), cranial (**B**), proximal (**C**) and distal (**D**) views. For measurements see Table 2.

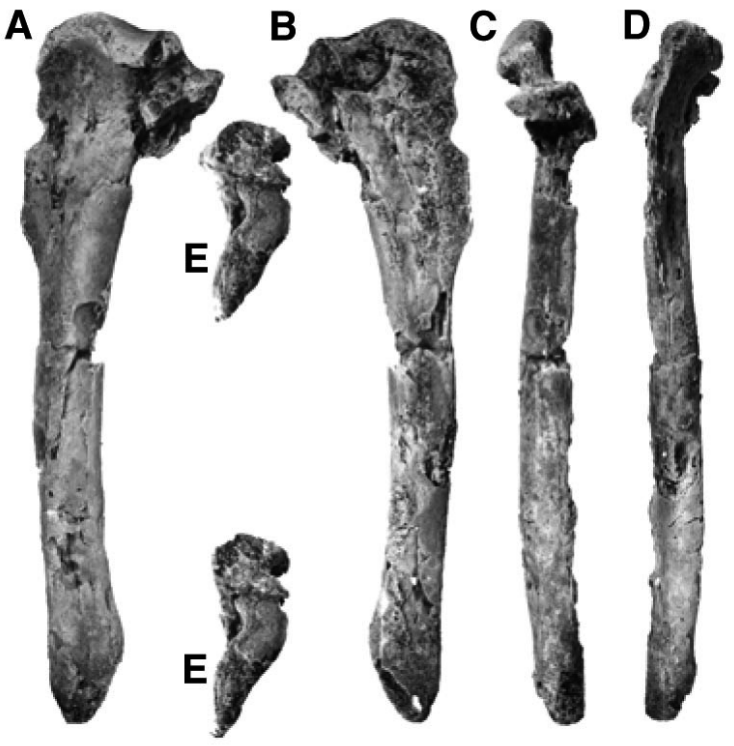

Fig. 21—Photographs of the holotype specimen of *Martinavis minor* (PVL 4046), proximal left humerus in caudal (**A**), cranial (**B**) and lateral (**C, D**) views. Stereo pairs of PVL 4046 in proximal view (**E**). For measurements see Table 2.

dorsally (Chiappe and Walker 2002). Descriptions and comments regarding some species of *Martinavis* were provided by Walker *et al.* (2007); note that *M. cruzyensis* is the type species of the genus (Walker *et al.* 2007) but is from the late Cretaceous of southern France.

Martinavis vincei Walker, Buffetaut and Dyke 2007

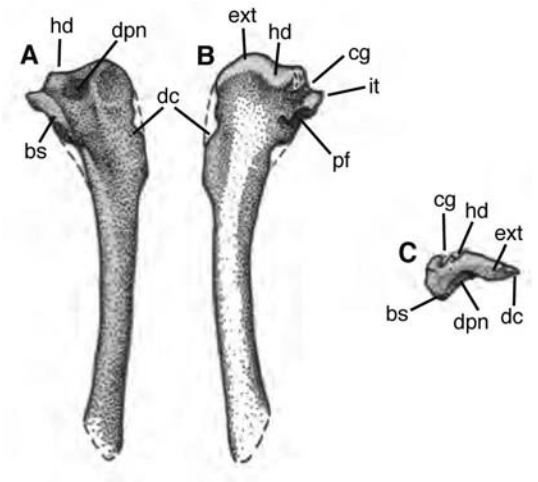

Fig. 22—Drawings of the holotype specimen of *Martinavis minor* (PVL 4046), proximal left humerus, in cranial (**A**), caudal (**B**) and proximal (**C**) views. For measurements see Table 2.

Figures 17–18; Table 2

Holotype
Complete left humerus (PVL 4054) (Figs 17, 18A–D).

Paratype
Distal end of left humerus (PVL 4059).

Diagnosis
As noted by Walker *et al.* (2007), *M. vincei* is comparable in size to *M. cruzyensis* (ACAP-M 1957) but is more gracile and has a humerus with a more cranially angled bicipital crest, a capital groove with a deeper depression, and more distally enlarged internal and external cotylae.

Description and comments
PVL 4054 is the most complete enantiornithine humerus currently known from El Brete, and is about two-thirds the size of the large *Enantiornis* (Figs 17–18) In cranial view, this element is characteristically L-shaped but differs in that its bicipital crest is more cranially deflected (Fig. 18A–D). The craniodistal margin of the deltoid crest also differs in joining the shaft more gradually although there is a resemblance in the shape and position of a well-marked muscle scar

Fig. 23 (above)—Photographs of the holotype specimen of *Martinavis whetstonei* (PVL 4028), proximal left humerus, in cranial (**A**), caudal (**B**) and lateral (**C, D**) views. Stereo pairs of PVL 4028 in proximal (**E**) view. For measurements see Table 2.

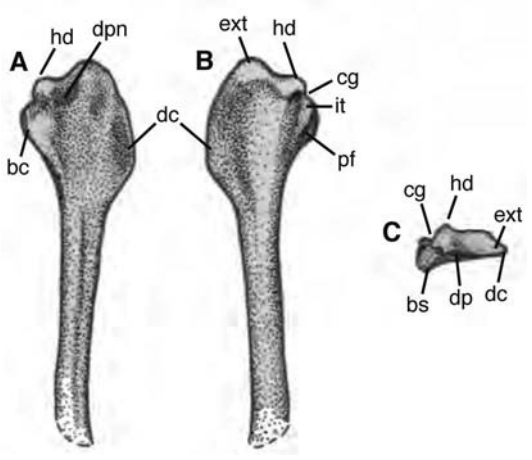

Fig. 24 (left)—Drawings of the holotype specimen of *Martinavis whetstonei* (PVL 4028), proximal left humerus, in cranial (**A**), caudal (**B**) and proximal (**C**) views. For measurements see Table 2.

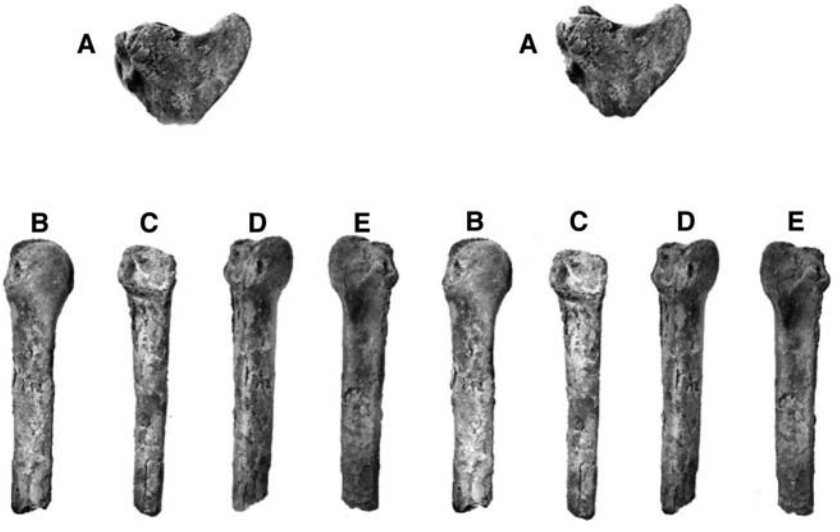

Fig. 25—Stereo photographs of PVL 4032, distal end of right ulna, referred to *Martinavis* sp. in distal (**A**), medial (**B**), cranial (**C**), caudal (**D**) and lateral (**E**). For measurements see Table 2.

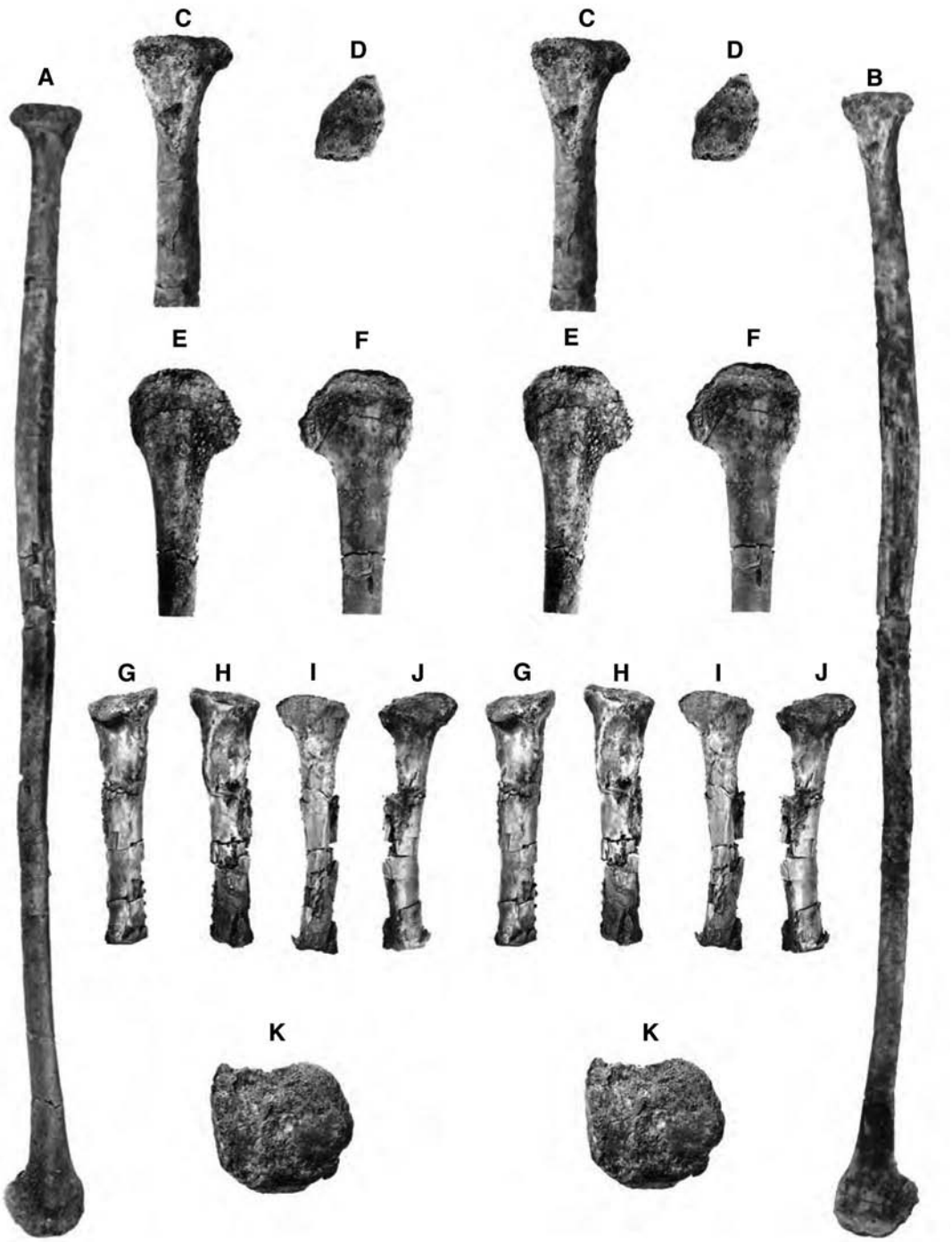

Fig. 26—Photographs of fossil specimens referred to *Martinavis* sp.: PVL 4056: complete right radius in dorsal (**A**) and ventral (**B**) views; proximal end in ventral (**C**) and proximal (**D**) views; distal end in dorsal (**E**) and ventral (**F**) views. PVL 4032, left tibiotarsus: in caudal (**G**), cranial (**H**), lateral (**I, J**) and proximal (**K**) views. **C–K** are stereo pairs; for measurements see Table 2.

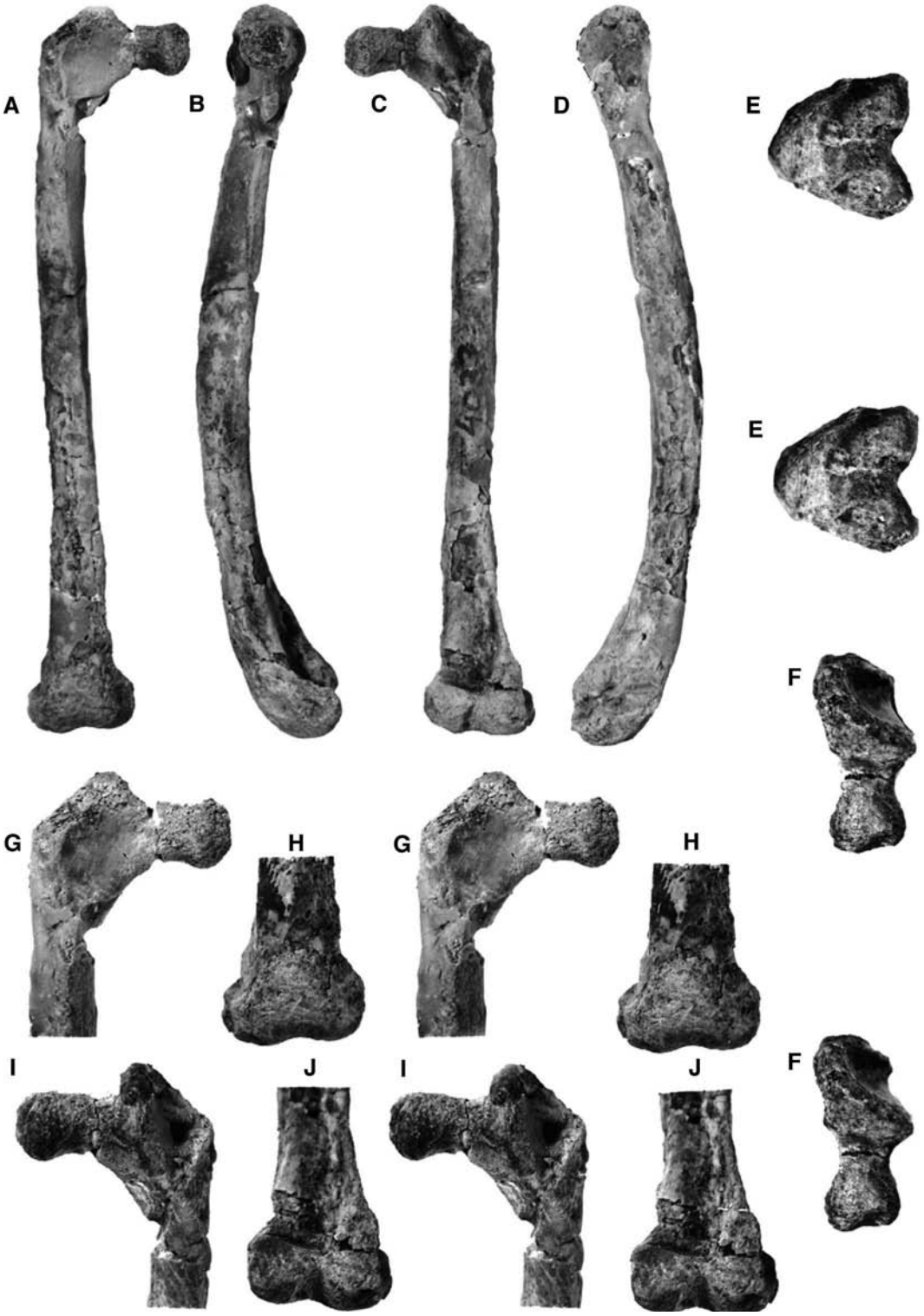

Fig. 27—Photographs of fossil material referred to *Martinavis* sp.: PVL 4037, complete right femur in cranial (**A**), medial (**B**), caudal (**C**), external (**D**), distal (**E**) and proximal (**F**) views (**E–F** in stereo pairs). Cranial view of proximal end (**G**), cranial view of distal end (**H**), caudal view of cranial surface (**I**), caudal view of distal end (**J**) (**G–J** in stereo pairs). For measurements see Table 2.

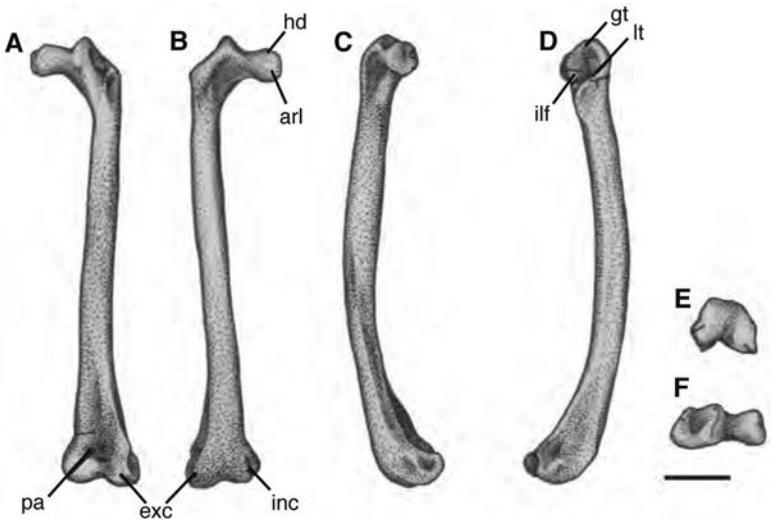

Fig. 28—Drawings of fossil material referred to *Martinavis* sp.: PVL 4037, complete right femur in caudal (**A**), cranial (**B**), lateral (**C, D**) distal (**E**), and proximal (**F**) views. For measurements see Table 2.

running down the lateral margin of the deltoid crest (Fig. 18). In caudal view, the proximal end differs considerably from *Enantiornis* in the possession of a much wider pneumatic fossa and no perforation of the internal tuberosity. Both *Enantiornis* and *Martinavis* lack a pneumatic fossa in the humeral head (cf. Figs 11 and 18).

Distally, the two genera cannot be compared in detail because of excessive damage to this region seen on elements currently referred to *Enantiornis* (Figs 5D–G); however, in *M. vincei* the ectepicondyle and entepicondyle in caudal view are distinctly rounded and lack distinct tricipital grooves (Fig. 17). Situated between the two condyles there is a deeply excavated

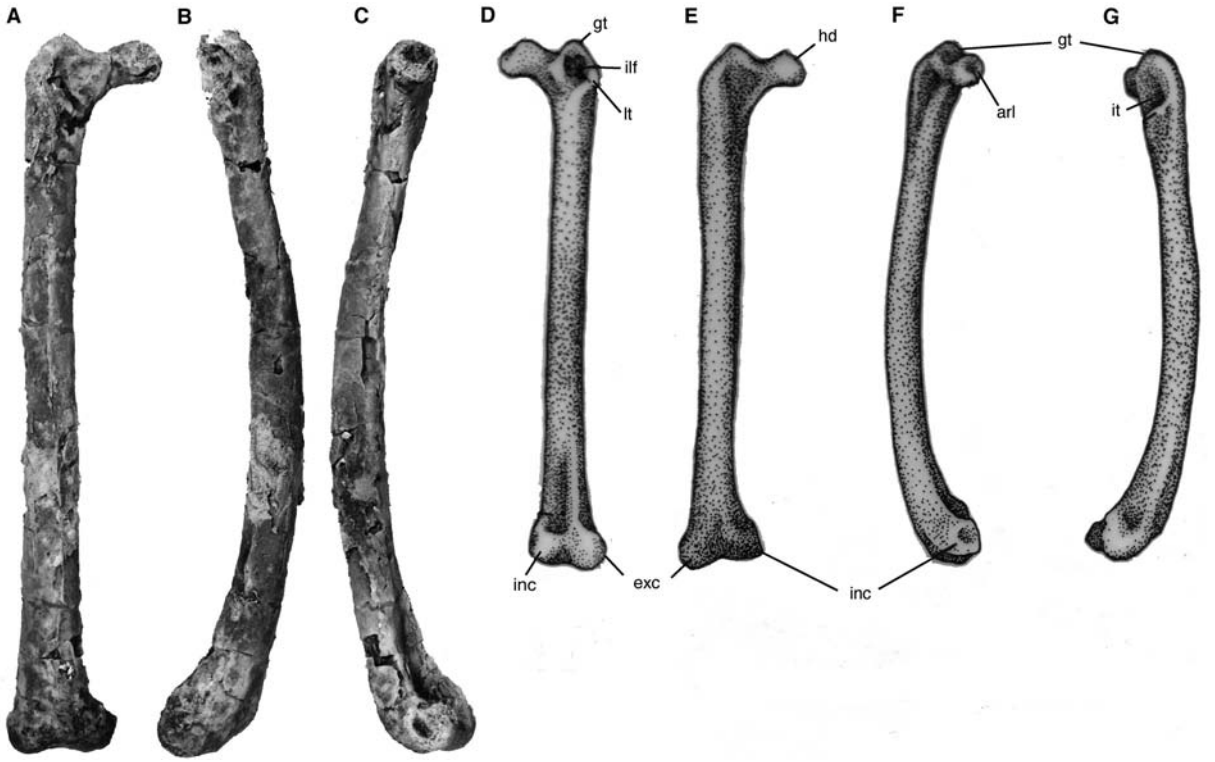

Fig. 29—Photographs of specimens referred to *Martinavis* sp.: complete right femur (PVL 4036) in cranial (**A**) and lateral (**B, C**) views. Drawings of PVL 4036, complete right femur in caudal (**D**), cranial (**E**) and lateral views (**F, G**). For measurements see Table 2.

Fig. 30—Photographs of specimens referred to *Martinavis* sp.: proximal end of right ulna (PVL 4044) in dorsal (**A**) and ventral (**B**) views; right femur (PVL 4038) in cranial (**C**) and caudal (**D**) views. For measurements see Table 2.

olecranal fossa, deepest towards the ectepicondyle. On the distal end of this element in cranial view, the ectepicondylar and entepicondylar prominences are well-developed (Fig. 17). The internal condyle is not expanded and thus differs from the bulbous condition seen in most modern birds. The external condyle also differs from neornithines in being less inflated and more transversely orientated.

Martinavis saltariensis sp. nov.
Martinavis sp. Walker, Buffetaut and Dyke 2007
Figures 19–20; Table 2

Etymology
The specific name is taken from Salta, the Argentine province where the El Brete collection was excavated in the 1970s.

Holotype
Incomplete left humerus (PVL 4025), lacking the median ridge (Figs 19–20). This specimen is crushed craniocaudally and was referred to as *Martinavis* sp. by Walker *et al.* (2007).

Diagnosis
As noted by Walker *et al.* (2007), this species is similar to its El Brete contemporary *M. vincei* and the French *M. cruzyensis* (ACAP-M 1957) but is smaller (Figs 19–20), while the latter is also more robust. The bicipital crest of PVL 4025 is less cranially inclined and the distal extremity of the deltoid crest meets the shaft more abruptly than in the other species of this genus. There is also no depression present in the capital groove and the base of the pneumatic fossa is deeper and broader; the internal border of the shaft proximal to this fossa is more gently sloped (Fig. 20). *M. saltariensis* has a small entepicondyle, a more laterally positioned ectepicondyle and a more transversely orientated external condyle (Fig. 20) than either *vincei* or *cruzyensis* (Walker *et al.* 2007).

Martinavis minor sp. nov.
Martinavis sp. Walker, Buffetaut and Dyke 2007
Figures 21–22; Table 2

Etymology
The specific name refers to the small size of this species, in comparison with the holotype of the genus.

Holotype
Distally imperfect right humerus (PVL 4046; Figs 21–22).

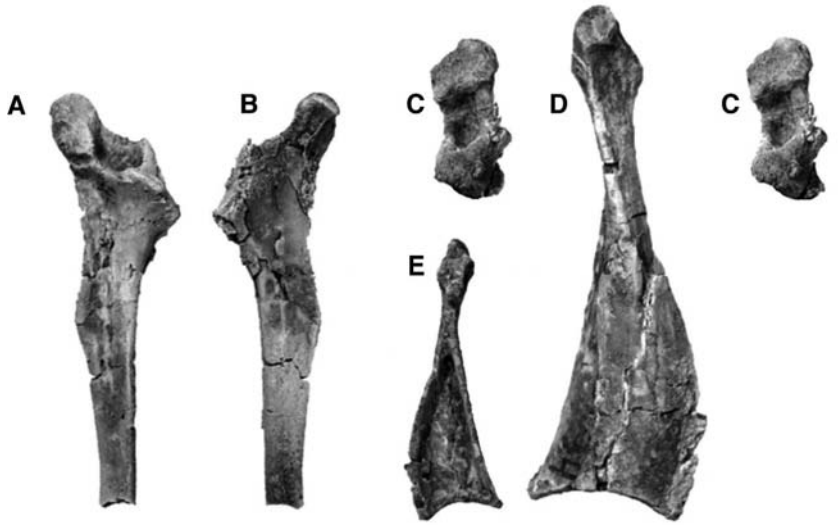

Fig. 31—Photographs of specimens referred to *Martinavis* sp.: scapula (PVL 4034) in medial (**A**), lateral (**B**) and ventral (**C**) views (the latter in stereo pairs); right coracoid (PVL 4034) in ventral (**D**) and dorsal (**E**) views. For measurements see Table 2.

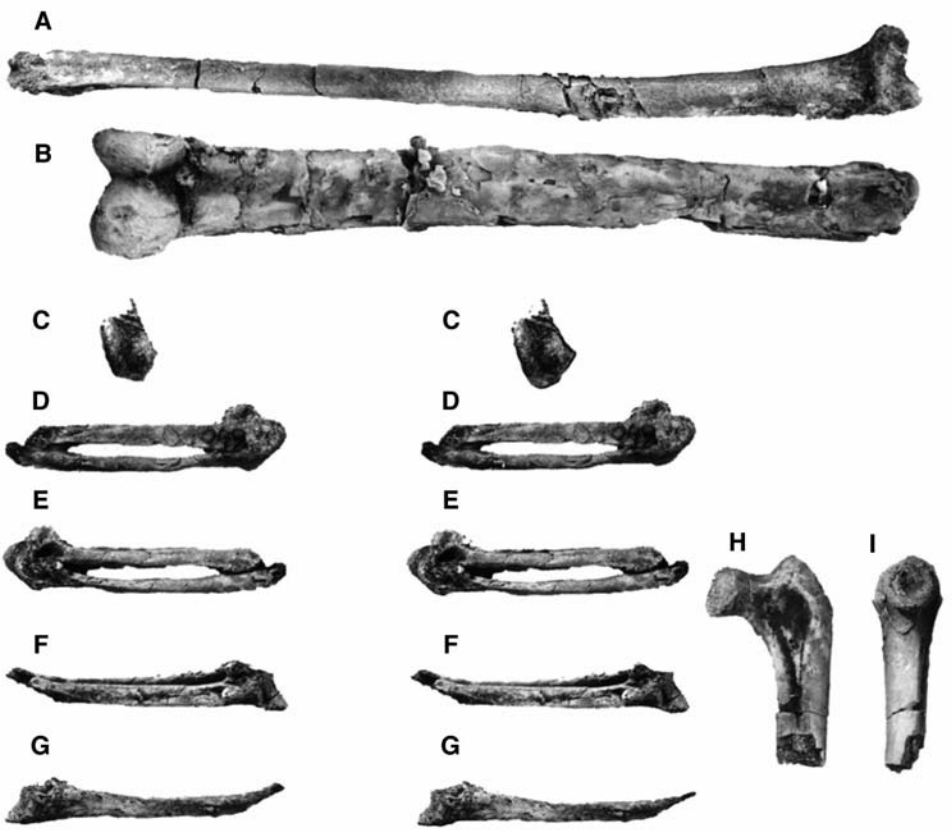

Fig. 32—Photographs of specimens referred to *Martinavis* sp: left ulna (PVL 4031) in dorsal view (**A**); distal end of tibiotarsus (PVL 4030) in anterior (**B**) view; right carpometacarpus (PVL 4049) in proximal (**C**), internal (**D**), external (**E**), dorsal (**F**) and ventral (**G**) views (**C–G** are stereo pairs); proximal end of left femur (PVL 4060) in anterior (**H**) and medial (**I**) views. For measurements see Table 2.

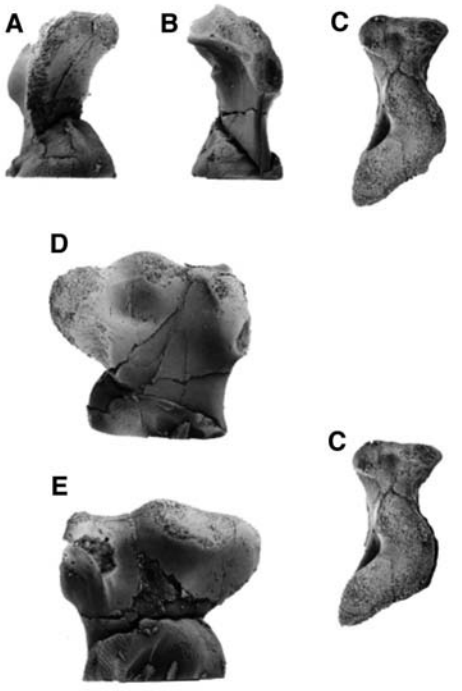

Fig. 33—Photographs of specimen referred to *Martinavis* sp.: proximal end of left humerus (KU-NM 37) in internal (**A**), external (**B**), proximal (**C**), cranial (**D**) and caudal (**E**) views (**C** as stereo pairs). For measurements see Table 2.

Diagnosis

This is a small species, about two-thirds the size of *M. vincei* and *M. saltariensis*. In addition to a clear size difference, this taxon differs from its contemporaries because the head of its humerus is less notched on its cranial surface and the external tuberosity less bulbous in proximal view (Fig. 22).

Description and comments

This element closely resembles corresponding bones referred to *M. vincei* and *M. saltariensis* but is about one-third smaller. Such a large difference in relative size likely precludes individual variation as well as the possibility that this element is part of a growth series pertaining to one of the two larger species (although this cannot be ruled out). In addition, it has not been possible to detect any sign of immaturity on this element (e.g., surface pitting or incomplete ossification of articulation surfaces). Compared to *M. vincei* (PVL 4054), the proximal humerus of *M. minor* has a less notched external tuberosity (Fig. 22). In caudal view, the deltoid crest—although broken—would have met the shaft gradually along its distal margin, while the area below the internal tuberosity slopes sharply away towards the medial margin of the shaft (Fig. 22). A deep depression within the capital groove is absent in this

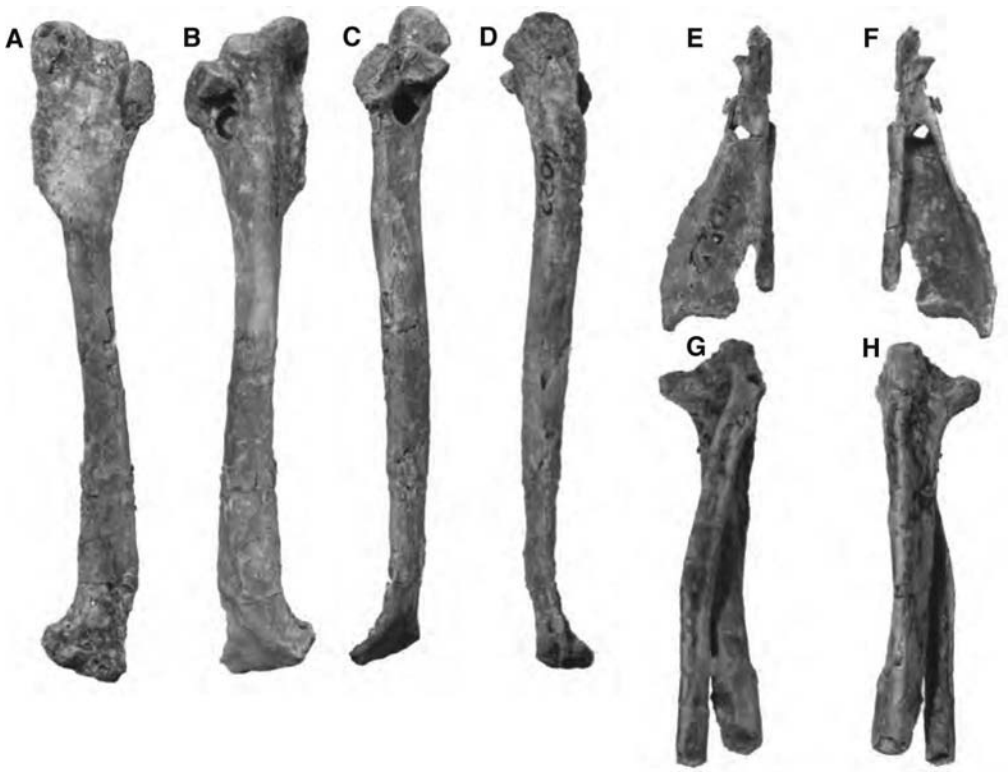

Fig. 34—Photographs of the holotype specimen of *Elbretornis bonapartei* (PVL 4022): left humerus in cranial (**A**), caudal (**B**), internal (**C**) and external (**D**) views; incomplete right coracoid in ventral (**E**) and dorsal (**F**) views; right ulna and radius in cranial (**G**) and caudal (**H**) views. For measurements see Table 2.

taxon and the shaft, distal to the pneumatic fossa, is more rounded (Fig. 22).

Martinavis whetstonei sp. nov
Martinavis sp. Walker, Buffetaut and Dyke 2007
Figures 23–4; Table 2

Etymology
This species is named in honour of K.H. Whetstone who gave C. Walker considerable encouragement to publish a paper on these 'strange birds' in the early 1980s.

Holotype
Distally imperfect left humerus (PVL 4028; Figs 23–4).

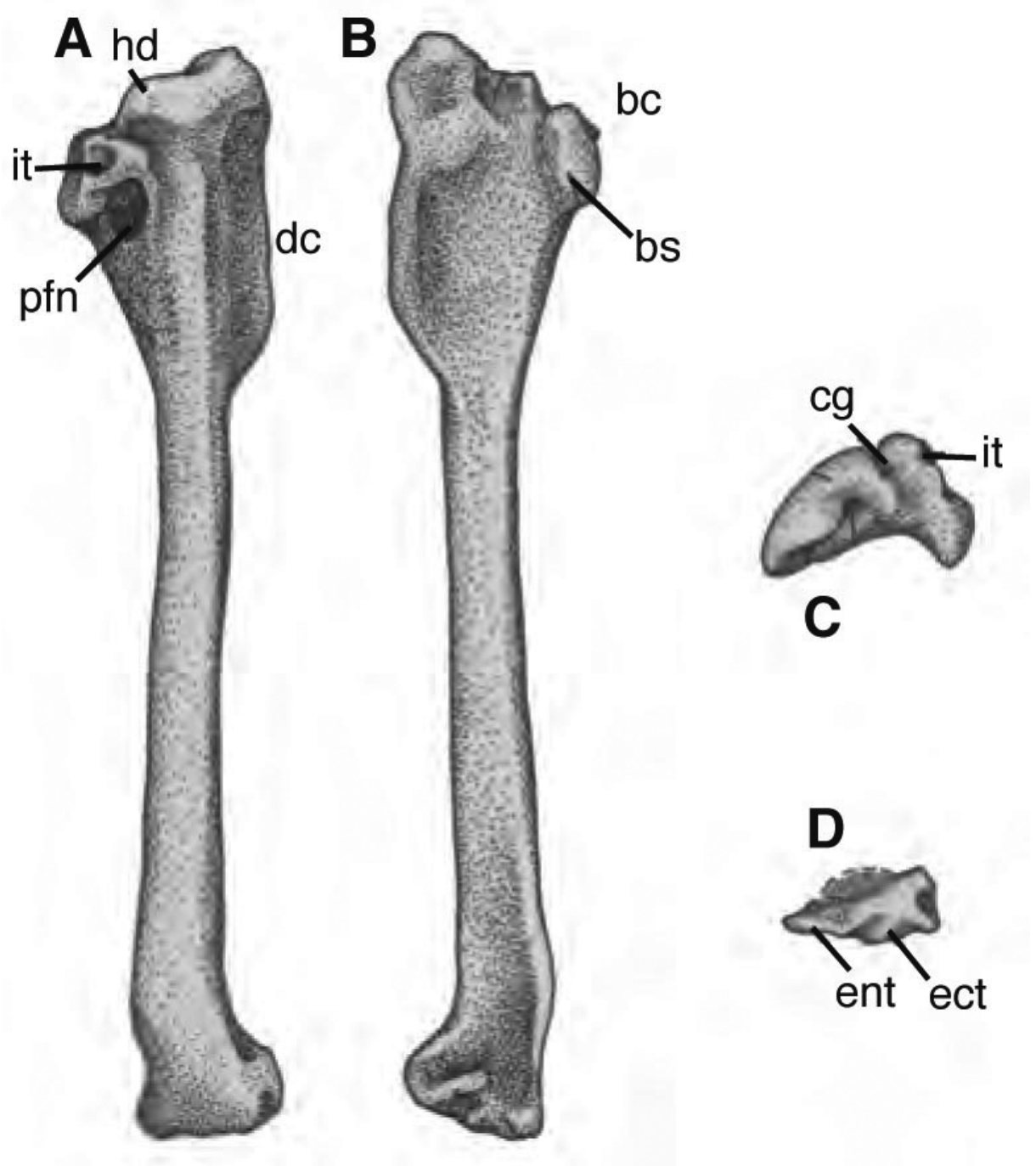

Fig. 35—Drawings of the left humerus that comprises part of the *Elbretornis bonapartei* holotype (PVL 4022) in caudal (**A**), cranial (**B**), proximal (**C**) and distal (**D**) views. For measurements see Table 2.

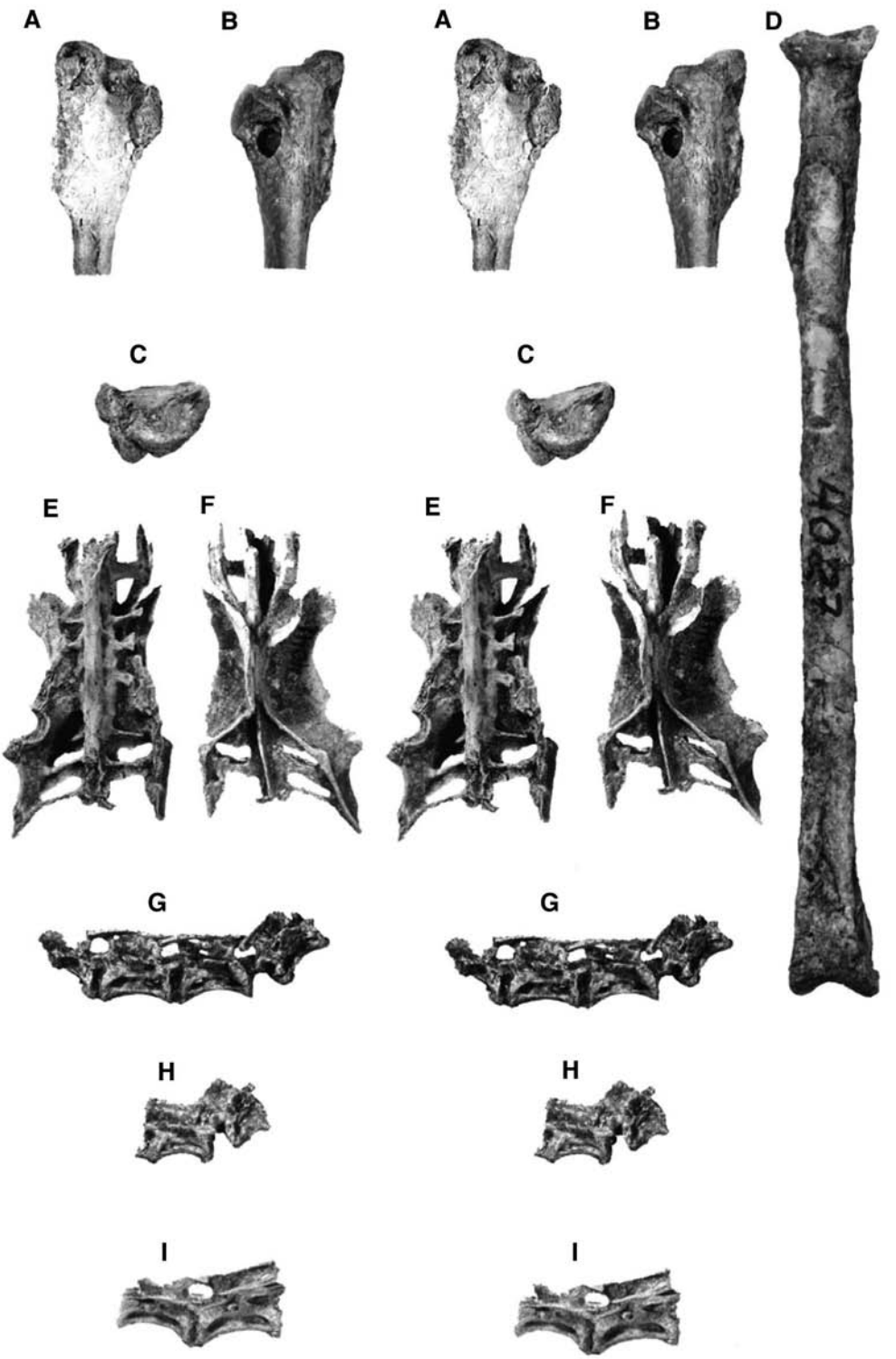

Fig. 36—Photographs of specimens referred to *Elbretornis*: stereo photographs of the *E. bonapartei* holotype humerus (PVL 4022) in cranial (**A**), caudal (**B**) and proximal (**C**) views; photograph of right tibiotarsus (PVL 4027) referred to *Elbretornis* sp. in caudal view (**D**); imperfect synsacrum (PVL 4041) in ventral (**E**) and dorsal (**F**) views (stereo pairs); series of thoracic vertebrae (PVL 4051) in lateral view (**G**); lateral views of single thoracic vertebra PVL 4041 (**H**) and PVL 4051 (**I**) (stereo pairs). For measurements see Table 2.

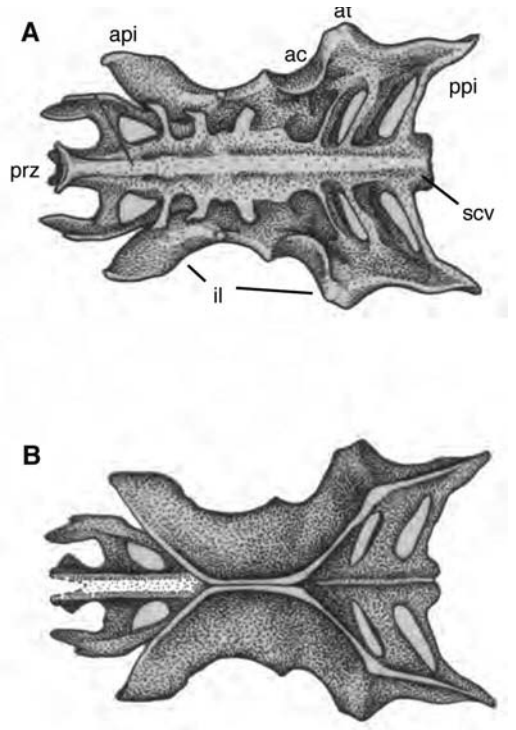

Fig. 37—Drawings of the synsacrum (PVL 4041) referred to *Elbretornis* sp. in dorsal (**A**) and ventral (**B**) views. For measurements see Table 2.

Diagnosis

This is another small euenantiornithine bird, close in size to *M. minor*. This taxon is differentiated by: the presence of a short deltoid crest; an internally positioned pneumatic fossa; a less cranially inclined bicipital crest; and a more bulbous external tuberosity (when compared with the other known species referred to this genus; see above).

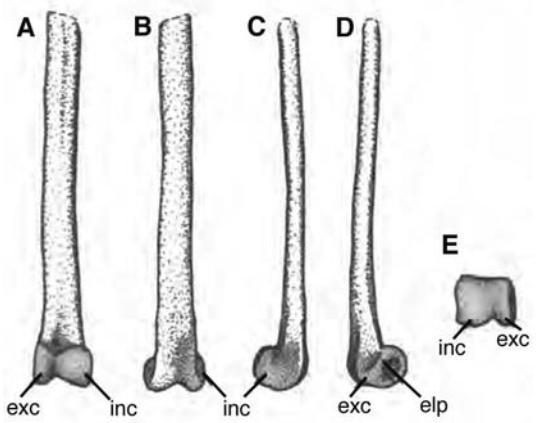

Fig. 38—Drawings of the incomplete proximal right tibiotarsus (PVL 4027) referred to *Elbretornis* sp. in cranial (**A**), caudal (**B**), medial (**C**), lateral (**D**) and distal (**E**) views. For measurements see Table 2

Description and comments

The humerus of this bird is similar in size to that described above for *M. minor* (cf. Figs 22 and 24), but differs in having a short and more rounded deltoid crest (Fig. 24) and a pneumatic fossa that is more internally positioned. When viewed anteriorly, the bicipital crest resembles *M. saltariensis* in that it is not markedly inclined cranially; in cranial view, the crest is similar to that of *Enantiornis* because it is less medially deflected than in the other described species of *Martinavis*. Further, the bicipital surface in this orientation is more bulbous than seen in *M. minor*, again approximating the condition seen in both *Enantiornis* and *M. saltariensis*.

Martinavis sp.
Figures 25–33; Table 2

Referred specimens

Distal end of right ulna (PVL 4032; Fig. 25), complete right radius (PVL 4056; Fig. 26A–F), complete left tibiotarsus (PVL 4032; Fig. 26G–K), complete right femur (PVL 4037; Figs 27–8), complete right femur (PVL 4036; Fig. 29), proximal end of right ulna (PVL 4044; Fig. 30A–B), complete right femur (PVL 4038; Fig. 30C–D), right scapula and coracoid (PVL 4034; Fig. 31), left ulna (PVL 4031; Fig. 32A), distal end of tibiotarsus (PVL 4031; Fig. 32B), proximal end of left femur (PVL 4060; Fig. 32H–I), right carpometacarpus (PVL 4049; Fig. 32C–G) (note that this element was formerly referred to *E. leali* by Chiappe and Walker 2002), and a proximal end of left humerus (KU-NM 37; Fig. 33A–E).

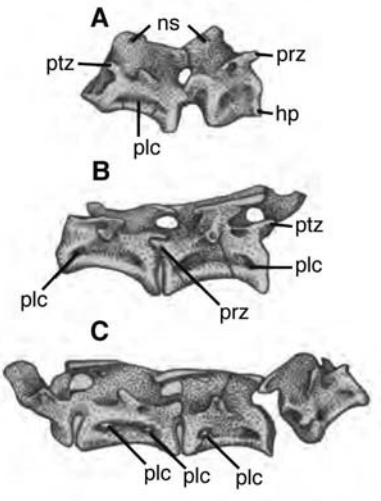

Fig. 39—Drawings of the thoracic vertebrae PVL 4041 (**A**) and PVL 4051 (**B–C**) referred to *Elbretornis* sp. in lateral views. For measurements see Table 2.

Description and comments

We have been unable to allocate the elements referred to above to other named euenantiornithines because of lack of specimen association. This did not, however, prevent Chiappe and Walker (2002) from referring the right carpometacarpus (PVL 4049; Fig. 32C–G) to *Enantiornis leali* even though it is much smaller than other known bones that certainly comprise this taxon (see above; e.g., PVL 4020; Fig. 9).

The scapula and coracoid (PVL 4034)—referred here to *Martinavis* sp.—are similar to *Enantiornis* but are much smaller. The scapula has a well-excavated preglenoid area, is steeply inclined dorsoventrally (Fig. 31A–C), and bears a wider notch in its medial wall just anterior to the coracoid facet. The coracoid has a distinct dorsal foramen situated in its blade rather than in the neck (as in *Enantiornis* and in one specimen described from the Cretaceous of France by Buffetaut (1998)); its lateral margin appears to be more convex, and does not form a ridge before flattening to become the blade (Fig. 31D–E). The isolated humerus (KU-NM 37) is slightly larger than that of *Enantiornis* and resembles the morphology seen in *M. saltariensis*, particularly in the area of the pneumatic fossa which is wide and lacks a pneumatised foramen (Fig. 33). On the proximal end of this element, the capital groove is wide and the medial crest is short, as in *M. saltariensis*.

One of the uncrushed distal parts of ulnae (PVL 4032) is similar in its morphology to other enantiornithine and extant (neornithine) birds in that it has a rounded external condyle, a small internal condyle, a distally located radial depression, and a well-marked carpal tuberosity (Fig. 25). Although also somewhat similar in its overall shape when compared to *Enantiornis* (PVL 4035), this bone lacks a distinct distal foramen. Nevertheless, PVL 4032 matches in size with humeri referred to *M. vincei* (see above) while the other ulna referred here (PVL 4031; Fig. 32A) is morphologically similar but its external condyle is not deflected proximally towards the olecranon. PVL 4056 is a virtually uncrushed right radius with a clearly semi-lunate proximal end (Fig. 26A–F) and a flat humeral facet (as opposed to 'cup-shaped' as is the case in extant birds). The distal end of this element is rounded and bears a deep ulnar depression, lending a 'spoon-shape' to this articulation. Caudally, there is no indication of a tendinal groove on this element but this may be an artefact of preservation; its lateral expansion differs from *Enantiornis* (Fig. 8) in that it is more rounded and less hooked.

The two well-preserved femora (PVL 4037 and PVL 4038) referred here to *Martinavis* sp. are tapered, long and slender (Figs 27–8 and 30C–D). PVL 4037 has a marked head set on a long neck that is orientated at right angles to its shaft, and a greater trochanter situated almost above the distal internal condyle. The lateral wall of this condyle is compressed while the iliac facet is angled medially onto the wall of the greater trochanter. A lesser trochanter is present, but this is reduced to a small, very thin and laterally placed blade. The distal condyles are level with one another but the fibular groove is weakly defined and is placed laterally with respect to the external condyle. The intercondylar fossa is not deeply excavated while the rotular groove is also indistinct and not impressed on the popliteal area; hence the distal extremity of this element remains rounded on its anterior surface. There is a distinct and marked depression in the head of the femur for the attachment of the round ligament, as is the case in all enantiornithine and subsequent birds. PVL 4038 is similar in size to PVL 4037 but has a more markedly deflected dorsal inflection to its head and neck, and its greater trochanter is less inclined medially (Fig. 30C–D). This element also has a thicker and straighter shaft, but these could also be a result of crushing.

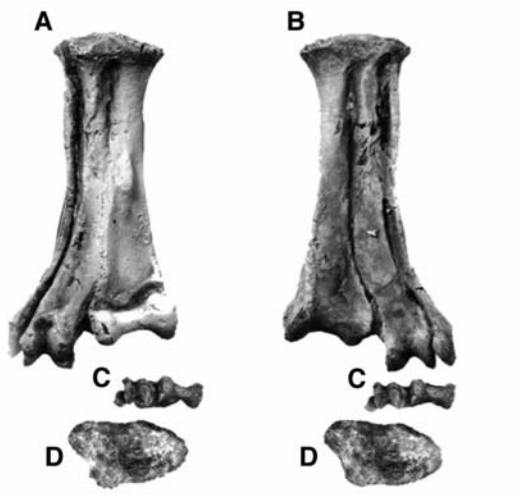

Fig. 40—Holotype specimen of *Yungavolucris brevipedalis* (PVL 4053) Chiappe 1993. Photographs of complete right tarsometatarsus in dorsal (**A**), plantar (**B**), distal (**C**) and proximal (**D**) views. For measurements see Chiappe (1993).

A third femur (PVL 4060) tentatively referred here to *Martinavis* sp. (Fig. 32H–I) comprises just the head and a fragment of shaft. This is enough, however, to show that this element is a miniature version of PVL 4038 (Fig. 30C–D); its head and neck are similarly inclined and the greater trochanter of this bone is more angled than is the case in PVL 4037 (Figs 27A–F, 28A–F). Based on size alone, this bone could feasibly belong either to *M. minor* or *M. whetstonei*; on the other hand, PVL 4060 could feasibly be a juvenile of one of the larger species even though there is no indication of immaturity.

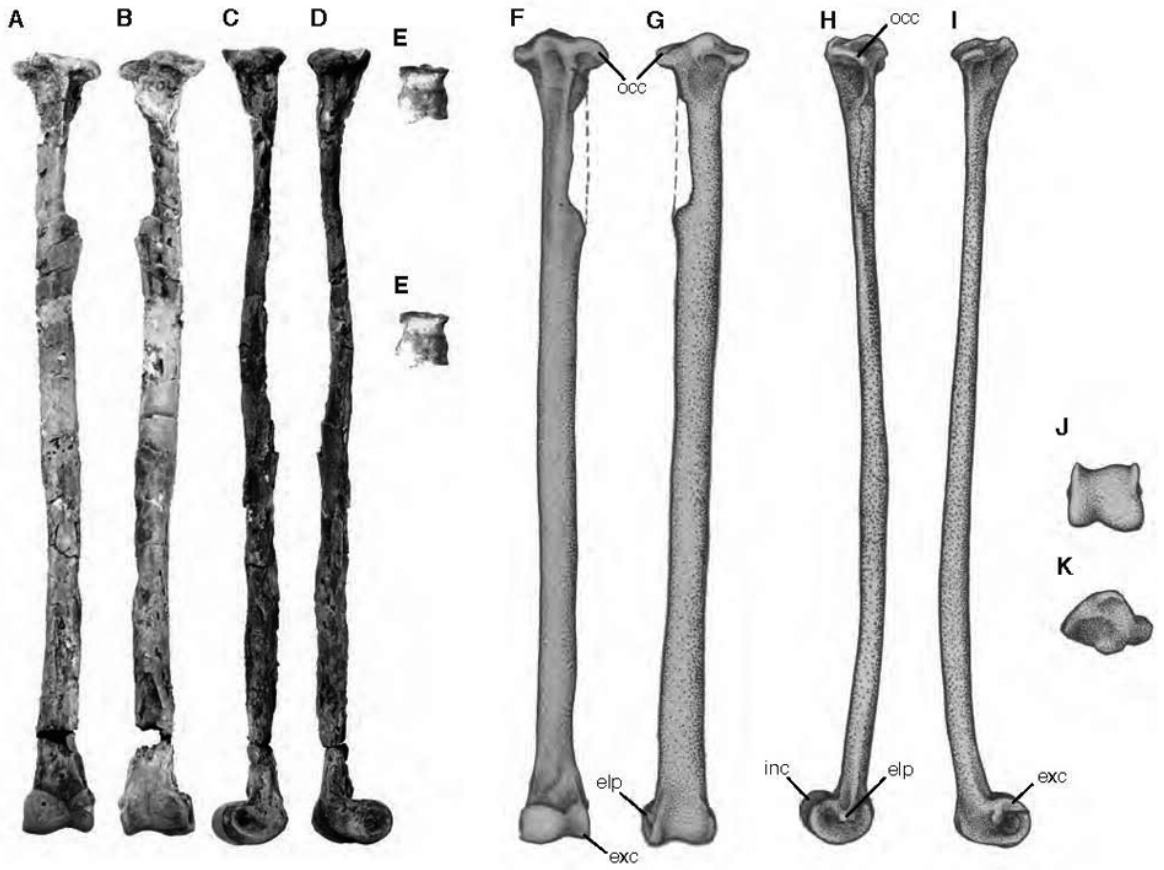

Fig. 41—Left tibiotarsus that comprises part of the holotype specimen of *Lectavis bretincola* (PVL 4021) Chiappe 1993: photographs in anterior (**A**), posterior (**B**), lateral (**C**) and medial (**D**) views; distal end as stereo pairs (**E**); drawings of PVL 4021 in anterior (**F**), posterior (**G**), lateral (**H**), medial (**I**), distal (**J**) and proximal (**K**) views. For measurements see Chiappe (1993).

Fig. 42—Proximal portion of left tarsometatarsus that comprises part of the holotype specimen of *Lectavis bretincola* (PVL 4021) Chiappe 1993: photographs in anterior (**A**), posterior (**B**), lateral (**C**) and medial (**D**) views. For measurements see Chiappe (1993).

An isolated proximal end of a tibiotarsus (PVL 4032) is referred here to *Martinavis* sp. (Fig. 26G–J). This specimen is particularly interesting because it bears the same number as an ulna (PVL 4032; see Table 1) and as such may provide a link between the hindlimb and forelimb elements of the El Brete euenantiornithines. In preserved anatomy, this bone is similar to PVL 4021, referred to *Enantiornis*; our tentative placement of this specimen within *Martinavis* is based purely on size. Referral of a similarly sized tibiotarsus (PVL 4033) by Chiappe and Walker (2002: Fig. 11.13) to another El Brete taxon, *Soroavisaurus australis*, however, complicates the possible synonymy of these birds (Walker *et al*. 2007; see below).

Elbretornis gen. nov.
Figures 34–9; Table 2

Etymology

Generic name taken from the ‘El Brete’ locality, Salta Province, Argentina.

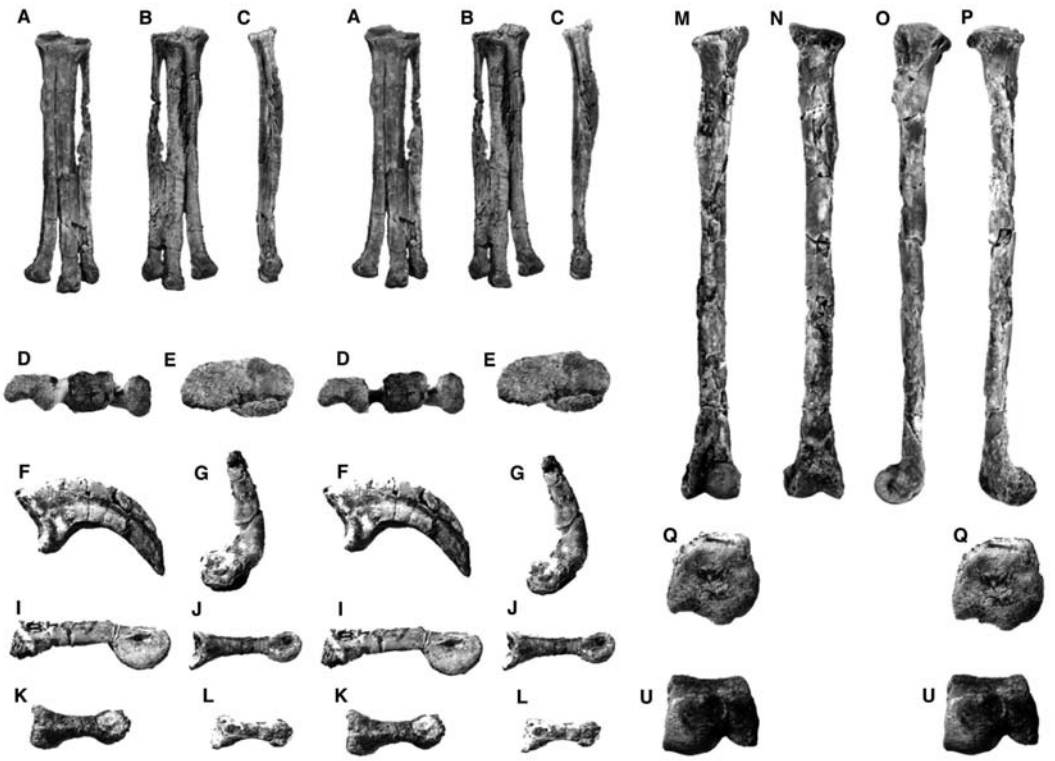

Fig. 43—Left tarsometatarsus referred to *Soroavisaurus australis* (PVL 4048) by Chiappe (1993): photographs in dorsal (**A**), plantar (**B**), lateral (**C**), distal (**D**) and proximal (**E**) views alongside associated claw (**F**) and phalanges (**G–L**) (all stereo pairs). Complete right tibiotarsus (PVL 4033) referred to *Soroavisaurus australis* by Chiappe and Walker (2002): photographs in cranial (**M**), caudal (**N**), medial (**O**), lateral (**P**), proximal (**Q**) and distal (**U**) views. For measurements see Chiappe (1993) and Chiappe and Walker (2002).

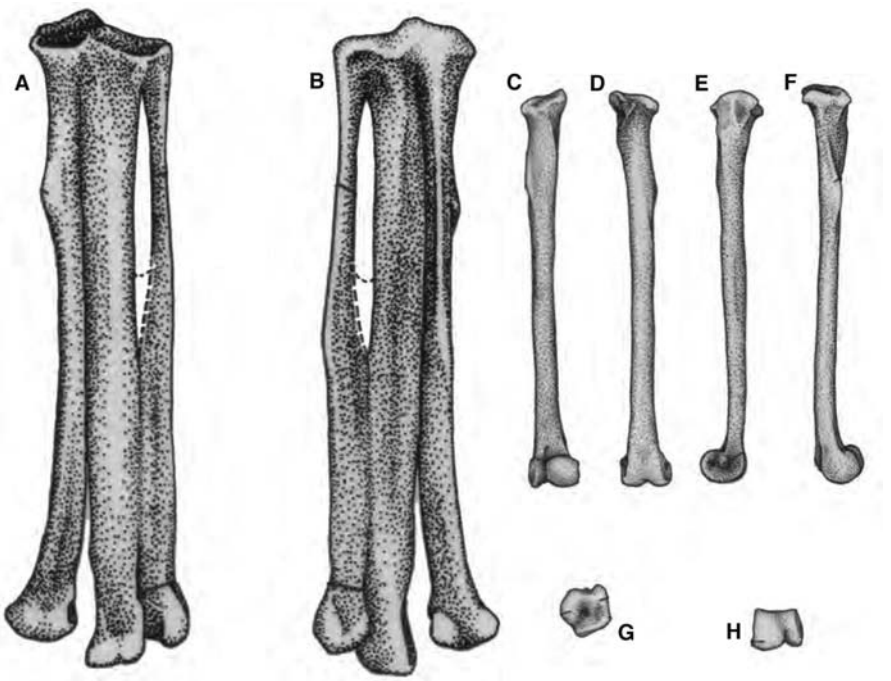

Fig. 44—Drawings of PVL 4048 in dorsal (**A**) and plantar (**B**) views. For images of the holotype specimen of *Soroavisaurus australis* (PVL 4690), see Chiappe (1993: Fig. 7). Drawings of complete right tibiotarsus (PVL 4033) in cranial (**C**), caudal (**D**), medial (**E**), lateral (**F**), proximal (**G**) and distal (**H**) views. For measurements see Chiappe (1993).

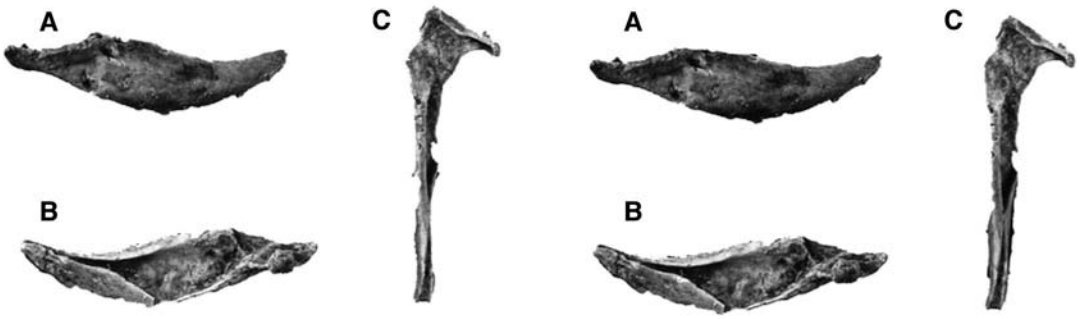

Fig. 45—Photographs of PVL 4698, posterior portion of lower jaw, in labial (**A**), lingual (**B**) and dorsal (**C**) views (stereo pairs). For measurements see Table 2 and Chiappe and Walker (2002). Note that this specimen, the only known skull element from El Brete, was not collected in association and is considered to be an indeterminate euenantiornithine in this paper.

Diagnosis

Elbretornis is an euenantiornithine bird that exhibits the following combination of characters: dorsal tuberculum of humerus strongly projected; mediolateral angle of proximal humerus slanted; large and deeply excavated pneumatic fossa on proximal end containing a deep, rounded and wide pneumatic foramen that undercuts the shaft; pneumatic foramen located distally within fossa; absence of an olecranon fossa on the caudal face of the distal humerus; condylus dorsalis bulbous and not angled transversely; absence of a bridge crossing the caudal portion of the shaft of the coracoid; well-developed and caudally orientated processus lateralis of coracoid; well-developed and concave sternal facet of coracoid turned somewhat onto the dorsal face; very large circular foramen nervi supracoracoidei that opens into the dorsal fossa of the coracoid; external cotyla of ulna deep and cup-shaped; ulna shorter than humerus; radius two-thirds the width of the ulna.

Elbretornis bonapartei sp. nov.
Figures 34–6; Table 2

Etymology

Species name in honour of Jose Bonaparte in recognition of his outstanding work on the Mesozoic vertebrate faunas of Argentina. J. Bonaparte directed the original field expeditions at El Brete (1974–6; Chiappe 2007) and loaned specimens for study to C.A. Walker in the 1970s (Walker *et al.* 2007).

Holotype

Left humerus and associated right radius, ulna, scapula and coracoid (PVL 4022; Figs 34–6).

Diagnosis

As for genus, only currently recognised species.

Description and comments

Walker (n.d.) originally intended to refer a number of additional postcranial elements not associated with PVL 4022 to this taxon which included vertebrae, a synsacrum and a tibiotarsus; because subsequent work (Chiappe 1991, 1993) erected taxa from El Brete based on tarsometatarsal morphology, the association of additional elements that cannot be matched directly to the holotype is problematic (see below).

The shape of the PVL 4022 humerus (Figs 34A–D, 35A–D, 36A–C) is similar to other elements collected from El Brete (Walker 1981; Chiappe and Walker 2002; Walker *et al.* 2007). As in all enantiornithines, the shape of the head in proximal view is L-shaped (Walker 1981; Fig. 36C) and the bicipital crest is orientated cranially, as in *Martinavis* (Walker *et al.* 2007). PVL 4022 falls within the size distribution of humeri referred to the contemporary *Martinavis* (Walker *et al*. 2007). On the proximal end, the dorsal tuberculum projects well above the level of the head (caput humeri) in cranial view (Fig. 34A–B) to create a strongly slanted, mediolaterally angled shape. In the other El Brete taxa (i.e., *Enantiornis*—Chiappe and Walker 2007; *Martinavis*—Walker *et al.* 2007), and in other known enantiornithines with three dimensionally preserved humeri (e.g., *Gurilynia*—Kurochkin 1999), the head is rounded but it is not as angled proximally. A long and deep transverse ligamental groove excavates the caudal surface of the bicipital crest, as in the other El Brete humeri. The ventral tubercle is perforated by a proximodistal canal, as seen in PVL 4020 and PVL 4043 (specimens originally referred to *Enatiornis leali* by Walker 1981). This tubercle is projected caudally and is separated from the humeral head by a deep capital incision.

The humeral head of PVL 4022 is concave cranially and convex caudally and is undercut by a marked and deep fossa (Figs 34A–B, 35A–B). Inside this fossa, a large and oval-shaped pneumatic foramen perforates the

internal wall of the bone and extends deep into the shaft. The presence of a foramen in this area on the *Elbretornis* humerus, as well as its size and extent of pneumaticity, appears to be unique amongst known enantiornithines. The deltopectoral crest of PVL 4022 is well-developed, projected cranially and is approximately the same width throughout its length. Distally this crest joins the shaft at a gradual angle. The bicipital crest is developed as a cranial projection relative to the shaft surface in ventral view (Figs 34A, 35A).

The shaft of PVL 4022 is triangular, sloping sharply to both its medial and lateral edges (Figs 34A–C; 35A–B). In *Martinavis* these angles are less apparent making the shaft appear more rounded in cross-section. The major axis of PVL 4022, between the proximal and distal ends, is twisted and angled at about 40° (also seen in PVL 4054) even though this element has been subjected to distortion during preservation (Fig. 34A–D).

On its distal end, PVL 4022 is craniocaudally compressed, transversely expanded and bears a distally projected ventral epicondyle (Fig. 35D). No well-developed olecranon fossa is present on the caudal face (Chiappe and Walker 2002: Fig. 11.8), and the external condyle is bulbous and is not angled transversely (as in *Enantiornis* and *Martinavis*; Walker *et al.* 2007). A well-developed brachial depression is present on the cranial face; the distal condyles are elliptical (subrounded) and located cranially. The long axis of the dorsal condyle is orientated at a high angle with respect to the humeral axis (Chiappe and Walker 2002: Fig. 11.8), while the length of the long axis of the ventral condyle is less than the same measure of the dorsal condyle.

Although the coracoid of PVL 4022 is damaged at both extremities, this bone is nevertheless elongate with a triangular profile (Fig. 34E–F). The cranial end is laterally compressed; there is no bridge crossing this surface in dorsal view (Fig. 34F). The humeral articular facet (glenoid) is large and located dorsally with respect to the acrocoracoid process; this process is straight, rounded but not hooked while the procoracoid process is absent (as is the case in all other known enantiornithines; Fig. 34E–F). The dorsal surface is strongly concave, rounded, and displays a deep fossa that occupies almost the whole of this face (Fig. 34F). The supracoracoid nerve foramen is located centrally and is very wide and rounded. This foramen opens inside the broad dorsal fossa (also seen in PVL 4034, a coracoid associated with a scapula, referred above to *Martinavis* sp.). In almost all other enantiornithines for which the coracoid is known (including *Enantiornis*), this foramen is smaller, is located above, and is separated from the fossa by its cranial edge (Walker *et al.* 2007). The medial surface of the PVL 4022 coracoid bears a depressed, elongate and wide furrow that narrows cranially (Fig. 34F). The lateral process (sternocoracoid process) is present, broad and orientated caudally as a rounded 'boss'. The sternal facet is concave and well-developed on the caudal surface (although turned somewhat onto the dorsal face) and the lateral margin is distinctly convex.

The right scapula of PVL 4022 is badly damaged at both extremities and has what appears to be the remains of the glenoid area of the coracoid crushed onto it. Although broken caudally, this bone was shorter than its corresponding humerus. Despite having been compressed during preservation, the scapula is robust, broad, and may not have been markedly curved. On the costal surface of the blade there is a prominent longitudinal furrow; towards the cranial end of this furrow a small foramen is also present—a similar foramen is also seen in PVL 4034. The acromion process is projected less cranially than is the articular surface for the coracoid, while the cranial end is broad, robust and expanded. On the cranial surface there is a deep and distinct pit between the acromion and the humeral articular facet.

The radius and ulna of PVL 4022 are crushed and cemented together by a matrix (Fig. 34G–H); the radius lacks both articulations while the ulna lacks its distal end. Although broken distally, the ulna was clearly shorter than the humerus while the radius measures about two-thirds the width of the ulna. On its proximal end, the cotylae of the ulna are widely separated by a deep groove (Fig. 34; the dorsal cotyla of PVL 4022 is deep and cup-shaped, more so than specimens attributed to *Enantiornis leali* (Walker 1981; Chiappe 1996; Chiappe and Walker 2002)). The incomplete radius bears a groove on its ventrocaudal surface.

Elbretornis sp.

Figures 37–9; Table 2

Referred specimens

Isolated dorsal vertebrae (PVL 4041, PVL 4047, PVL 4051), synsacrum, possibly associated femur and rib fragment (PVL 4041), and incomplete right tibiotarsus (PVL 4027).

Description and comments

The three vertebrae (PVL 4041, PVL 4047, PVL 4051) could have formed part of a series from a single individual, with the exception of PVL 4047 which is too large to be associated (Figs 36G–I, 39). For the

same reason, vertebrae PVL 4041 is likely associated with the synsacrum that bears the same number (Fig. 37). Each of these dorsal vertebrae has elongate, rather platycoelous centra and elongate pleurocoels which are deepest anteriorly and posteriorly. These centra lack any major development of their hypapophyses and the posterior dorsal margins of their neural spines are bifurcate, thus producing an area of articulation with the preceeding vertebra. Similarities are apparent, however, in the structure of the neural spines—these are long, low and blade-like contacting their neighbors.

The fused series of elements that comprise the synsacrum (PVL 4041) includes both ilia and a set of sacral vertebrae that have been distorted during fossilisation (Fig. 37; Chiappe and Walker 2002: Fig. 11.11). This synsacrum is referred to *Elbretornis* on the basis of its size; it is too small to be referred to *Enantiornis*, *Lectavis*, *Yungavolucris* or *Soroavisaurus* (see below), and too large to be referred to *Martinavis*. Compared to a set of elements referred to *Enantiornis* sp. (PVL 4042; Fig. 15), PVL 4041 has a similarly shaped anterior blade (deep, rounded and concave) and a posterior process that is narrow and prong-like (Fig. 37). A distinct supracetabular tubercle is present above the acetabulum on the dorsal edge of the iliac blade. Another feature seen in PVL 4041 that is not apparent in PVL 4042 (Fig. 15) is an antero-posteriorly running flange positioned medially to the anterior blade of the ilium and fixed at right angles to the transverse process of the anterior sacral vertebrae (Fig. 37). This flange, which may be part of the transverse process, is notched anteriorly thus indicating a possible articulation with the preceeding vertebra (Fig. 37; see Chiappe and Walker 2002: Fig. 11.11). Posteriorly, this flange is also fused to the following transverse process.

It is not possible to determine the exact number of vertebrae that are incorporated into this sacral sequence, but there appear to be at least eight (Fig. 37). The tail in this bird does appear to have been reduced, not elongate as is the case in more basal avians (*Archaeopteryx*); the presence of an avian pygostyle cannot be eliminated. In dorsal view, the shield is not developed behind the acetabulum (as in *Enantiornis*; Fig. 15); PVL 4041 does not have such a broad medial expansion of the dorsal edge of the ilium (Fig. 37).

A femur, rib fragment and dorsal vertebrae are apparently associated with this synsacrum by number (PVL 4041; Table 1). In most respects, the femur resembles those tentatively referred to *Martinavis* sp., but there are a number of differences in the region of the internal condyle which is flange-like posteriorly and bears a deep depression on its medial surface. This femur also has a long and elongate scar that runs down its lateral surface and bears a tubercle on its anterior margin. The tibiotarsus (PVL 4027; Fig. 38) is damaged by erosion and crushing during preservation and provides few useful characters; it is tentatively referred here to *Elbretornis* sp. on the basis of its size and style of preservation.

Yungavolucris Chiappe 1993
Yungavolucris brevipedalis Chiappe 1993
Figure 40; Table 2

Holotype
Nearly complete right tarsometatarsus (PVL 4053; Fig. 40) (Chiappe 1993: Fig. 2).

Paratypes
Incomplete right tarsometatarsi (PVL 4040 and PVL 4692), incomplete left tarsometatarsus (PVL 4052) and a distal trochlea of right metatarsals II and III (PVL 4268) (Chiappe 1993: Figs 3 and 4). These elements were listed as referred specimens by Chiappe (1993); for additional illustrations and descriptions of these elements see Chiappe (1993) and Chiappe and Walker (2002).

Lectavis Chiappe 1993
Lectavis bretincola Chiappe 1993
Figures 41–2; Table 2

Holotype
Associated left tibiotarsus and incomplete tarsometatarsus (PVL 4021; Figs 41, 42) (Chiappe 1993: Figs 5, 6). For additional illustrations and a description of this element see Chiappe (1993) and Chiappe and Walker (2002).

Soroavisaurus Chiappe 1993
Soroavisaurus australis Chiappe 1993
Figures 43–4; Table 2
1985 *Avisaurus* sp. (Brett-Surman and Paul 1985)

Holotype
Left tarsometatarsus (PVL 4690) (Chiappe 1993: Fig. 7).

Paratype
Left tarsometarsus with proximal and distal phalanges of digit I and four intermediate phalanges (PVL 4048; Figs 43, 44). This element was listed as a referred specimen by Chiappe (1993); for additional illustrations and descriptions of these elements, see Walker (1981), Brett-Surman and Paul (1985), Chiappe (1992, 1993), Chiappe and Calvo (1994) and Chiappe and Walker (2002).

Euenantiornithine indet.
Figure 45; Table 2

Referred specimen
Posterior (caudal) portion of a right lower jaw ramus lacking the region anterior to the surangular (PVL 4698; Fig. 45) (Chiappe and Walker 2002: Fig. 11.3C–E).

Description and comments
This portion of a lower jaw is upturned in lateral view (Chiappe and Walker 2002) and has a strongly concave dorsal margin. The retroarticular area is depressed and bears a short, rounded retroarticular process (Fig. 45). The posterior border is slightly notched and runs labiolingually before terminating in an elongate, hooked internal mandibular process that is projected anteriorly. Immediately anterior to the retroarticular area, two cups form the facets for the quadrates: these are separated by a round, transverse ridge. There is no external mandibular process. On the labial surface the convex-sided surangular is depressed anteriorly to below the anterior process (Fig. 45): the bone is perforated by a dorsal foramen, anterior to the rim of the articular surface. This bone is considered euenantiornithine because it was collected alongside the other elements described in this paper (and following Chiappe and Walker 2002). If this is the case, the element must be from one of the larger El Brete species—*Enantiornis*, *Martinavis*, or any of the three genera erected by Chiappe (1993).

Comparisons
Few Mesozoic birds are known that have a lower jaw preserved in three-dimensions. Compared to other birds, PVL 4698 superficially resembles the enantiornithine *Gobipteryx* as well as hesperornithiforms and extant gaviiforms (loons) and columbiforms (pigeons and doves) in the shape and morphology of its articular surface. These birds all share a transversely orientated, labio-lingual ridge that divides the facets for the quadrates and have poorly developed external mandibular processes (Elzanowski 1981; Chiappe and Walker 2002). Supporting its enantiornithine affinities, PVL 4698 is similar to *Gobipteryx* (Elzanowski 1981) in the shape of its internal mandibular processes. Distinct from known mandibles of hesperornithiform birds, the foramen that perforates the surangular in PVL 4698 is situated posteriorly, away from the anterior margin of the fossa. Hesperornithiforms also differ from this element in that the posterior articulation facet for the quadrate condyle is placed above the dorsal edge of the ramus, rather than below as in other birds and PVL 4698 (Fig. 45).

Discussion

Because of the importance of the El Brete bird bones, it is surprising that so few publications have been devoted to this collection. Nevertheless, Walker's (1981) original view of these fossil remains has been borne out by subsequent discoveries from elsewhere in the world. Walker (1981) hypothesised that: (1) Enantiornithes would prove to be widespreadwith a likely global distribution in the Cretaceous (Fig. 2); and that (2) Enantiornithes would prove to be the most abundant group of Mesozoic birds with their range being restricted to the Cretaceous (Feduccia 1999, 2006; Zhang and Zhou 2000; Zhang *et al.* 2000; Chiappe and Walker 2002; Fountaine *et al.* 2005; Chiappe 2007; Chiappe *et al.* 2007).

Walker *et al.* (2007) provided a historical review of the El Brete collection (Table 1)—Chiappe (1991, 1992, 1993) and Chiappe and Walker (2002) added descriptions and interpretations of some of the known specimens subsequent to Walker (1981). We now know that at least four (and possibly as many as six) genera of euenantiornithines are represented in this collection of more than 60 largely isolated bones (Walker *et al.* 2007: p. 984) that comprise three distinctive 'tarsometatarsal' (Chiappe 1993; Chiappe and Walker 2002) and five 'humeral' morphotypes (Walker 1981; Walker *et al.* 2007). Two of these 'humeral' morphotypes were originally recognised by Walker (1981)—one as *Enantiornis*, the other unnamed but subsequently described as *Martinavis vincei* (Walker *et al.* 2007)—while three more are presented here (i.e., *M. saltariensis*, *M. whetstonei*, *M. minor*). Nevertheless, although we have provided a complete taxonomy and descriptions of the El Brete specimens known to us, at least two fundamental questions remain: (1) how can the disassociated fore and hindlimb elements from El Brete be reconciled with one another?; and (2) what can this important collection of Late Cretaceous birds add to our understanding of Mesozoic avian phylogeny and evolution? Although lots of articulated specimens of enantiornithine birds are now known (Fountaine *et al.* 2005), particularly from the Cretaceous of Spain and China (Sanz *et al.* 1995; Chiappe 2007), few of them are three dimensionally preserved. Certainly no fossil material presently exists that would allow us to corroborate the taxonomic hypotheses thus far presented on the basis of the El Brete collection. Thus, questions of taxon synonymy and (much more importantly) the association between forelimb and hindlimb elements must await the recovery of additional fossil material. While it seems likely that *Elbretornis* and *Enantiornis* comprise a clade (they share a number of derived features including a shorter ulna than humerus),

taken in combination with the absence of a large-scale phylogenetic hypothesis for enantiornithines (beyond the scope of this paper), discussion of the evolutionary significance of the El Brete specimens is currently limited.

We do know, however, that the morphology of some of the Argentine birds are mirrored in taxa from the other side of the world—Walker *et al.* (2007) recognised that the genus *Martinavis* has been collected from both the Late Cretaceous of Argentina (El Brete) and Southern France (Massecaps). In other words, very similar (congeneric) euenantiornithine birds were present on both Laurasia and Gondwana in the late Campanian–early Maastrichtian. Most other representatives of this lineage, indeed Mesozoic birds in general (Chiappe and Dyke 2002; Chiappe 2007), are known from just single localities (Fountaine *et al*. 2005). This distribution pattern is interesting because the presence of fossils with 'Gondwanan' affinities in the Late Cretaceous vertebrate faunas of south-western Europe has been reported before (Buffetaut 1989), most convincingly abelisaurid theropods (Buffetaut *et al.* 1988) and mawsoniid coelacanths (Cavin *et al.* 2005)—both of which occur at Massecaps together with *Martinavis*.

In addition to their paleobiogeographic significance, *Enantiornis* and *Elbretornis* provide us with important data that augment our understanding of euenantiornithine biology—both these El Brete birds possessed extremely pneumatised forelimb bones (as initially noted by Walker 1981). Birds in general are readily distinguished from other living vertebrates by a suite of familiar morphological traits, including their aerodynamically functional feathers. Less familiar—though equally distinctive—is the avian respiratory system, in which a set of expandable air sacs ventilate a rigid lung. It is this unique respiratory system that allows birds to meet the metabolic challenges of their defining characteristic—flight. As part of this unique system, growths of air sac epithelia (diverticulae) often invade the avian post-cranial skeleton. This is seen well-developed in very few Mesozoic taxa (perhaps because of the rarity of three-dimensional preservation)—the Jurassic *Archaeopteryx* had pneumatised vertebrae (Britt *et al.* 1998; Christiansen and Bonde 2000) while *Elsornis*, a euenantiornithine from the Late Cretaceous of the Gobi Desert (Mongolia), had a pneumatised furcula (Chiappe *et al.* 2007). *Enantiornis* and *Elbretornis* are the first known examples of Mesozoic birds that certainly had pneumatised forelimbs—seen clearly in their preserved ulnae (*Enantiornis*) and humeri (*Elbretornis*). Such skeletal 'pneumaticity' probably has no direct respiratory role: the air sacs and their diverticulae are often minimally vascularised and thus virtually incapable of gaseous exchange (O'Connor and Claessens 2005). Rather, the concomitant mass reduction (up to 7–10%) has often been cited as an adaptation for flight (see for e.g., Cornell Lab of Ornithology 2004). We would also expect buoyancy in birds to be affected by the relative degree of skeletal pneumaticity (O'Connor 2004). As well as providing us with clearly diagnostic apomorphies for taxon differentiation, the deeply pneumatised forelimb bones of these El Brete enantiornithines raise interesting ecological questions: were *Enantiornis* and *Elbretornis* proficient flying birds? Or were they also adapted for a semi-aquatic mode-of-life? Certainly, the paleobiogeographic distribution of the contemporaneous *Martinavis* has led to suggestions that this bird could have been migratory (Walker *et al.* 2007) while some of the tarsometatarsal morphologies seen in these birds (e.g., *Yungavolucris*; Chiappe 1993; Chiappe and Walker 2002) are consistent with those seen in extant divers, such as penguins. We have a lot yet to learn about the biology of enantiornithines in general and the bizarre El Brete taxa in particular.

One thing is certain—since the work of Walker (1981) the number of known specimens and taxa of enantiornithine birds has ballooned (e.g., Fountaine *et al.* 2005; Walker *et al.* 2007). Students of avian evolution are working with more specimens discovered and described in the last fifteen years than were known for most of the preceding two centuries. However, in spite of this preponderance of fossils, fundamental questions in avian evolution still remain unanswered—for serious discussion is the question of avian lineage survivorship across the Cretaceous–Paleogene (K–Pg) extinction horizon. Although dominant during the latter half of the Mesozoic, and known from a fossil record that extends into the Campanian–Maastrichtian, enantiornithines did not survive this event (Feduccia 1999; Chiappe and Dyke 2002; Chiappe 2007) while the antecedents of all the extant lineages of birds (ornithurines) did: to adequately address the mechanisms of such apparently 'selective avian survivorship' adequate analysis of the fossil record from both sides of the K–Pg boundary is still required. El Brete taxa comprise just one important piece of this puzzle: we hope that this paper will, at least, provide others with a comprehensive, well-illustrated view of the diversity of these birds.

Acknowledgements

We thank Alexander Averianov, Eric Buffetaut, Luis Chiappe, Evgeny Kurochkin and Jingmai O'Connor for their kindness, support and for granting access to

unpublished data and especially Sandra Chapman for providing a great deal of help, support and advice over the years critical to Cyril Walker's work in London. Gareth Dyke also wishes to thank the two anonymous reviewers for their helpful comments and Matthew Parkes for his kind editorial support. This paper was in progress for more than twenty years: Jose Bonaparte loaned the El Brete collection to Cyril Walker in the 1970s and Jaime Powell (Universidad de Tucuman) provided additional photographs of specimens not available to Walker; Larry Martin wholeheartedly supported Walker's original research and (with his wife) provided much appreciated accomodation for Walker's extended stay in Kansas. As we have noted before, many of the original illustrations used in this paper (and Chiappe and Walker 2002) were rendered by KU-NM artists, while photographs were taken by Phil Crab and Phil Hurst under the guidance of Tim Parmenter of the photographic section (British Museum, Natural History). Judy Greenwood, Phil Hurst and Tim Parmenter provided a great deal of help and support with this project over the years and Julia Sigwart kindly drew Figure 4. Jose Bonaparte's visits to London were funded by the Frank M. Chapman Fund of the American Museum of Natural History while the most recent incarnation of this project was funded by University College Dublin (Seed Funding 2008) and Enterprise Ireland (Ulysses Programme 2003–04).

References

Baumel, J.J. and Witmer L.M. 1993 Osteologia. In J.J. Baumel, A.S. King, J.E. Breazile, H.E. Evans, and J.C. Vanden Berge (eds), *Handbook of avian anatomy: nomina anatomica avium*, 2nd edn. Publications of the Nuttall Ornithological Club 23, 45–132. Harvard. Nuttall Ornithological Club.

Bonaparte, J.F. and Powell, J.E. 1980 A continental assemblage of tetrapods from the Upper Cretaceous beds of El Brete, northwestern Argentina (Sauropoda-Coelurosauria-Carnosauria-Aves). *Mémoires de la Société Géologique de France* **139**, 19–28.

Brett-Surman, M.K. and Paul, G. 1985 A new family of bird-like dinosaurs linking Laurasia and Gondwanaland. *Journal of Vertebrate Paleontology* **5**, 133–8.

Britt, B.B., Makovicky, P.J., Gauthier, J. and Bonde, N. 1998 Postcranial pneumatization in *Archaeopteryx*. *Nature* **395**, 374–6.

Brodkorb, P.E. 1976 Discovery of a Cretaceous bird, apparently ancestral to the orders Coraciiformes and Piciiformes (Aves: Carinatae). *Smithsonian Contributions to Paleobiology* **27**, 67–73.

Buffetaut, E. 1989 Archosaurian reptiles with Gondwanan affinities in the Upper Cretaceous of Europe. *Terra nova* **1**, 69–74.

Buffetaut, E. 1998 First evidence of enantiornithine birds from the Upper Cretaceous of Europe: postcranial bones from Cruzy (Hérault, southern France). *Oryctos* **1**, 131–6.

Buffetaut, E., Mechin, P. and Mechin-Salessy, A. 1988 Un dinosaure théropode d'affinités gondwaniennes dans le Crétacé superieur de Provence. *Comptes Rendus de l'Académie des Sciences de Paris* **306**, 153–8.

Cavin, L., Forey, P.L., Buffetaut, E. and Tong, H. 2005 Latest European coelacanth shows Gondwanan affinities. *Proceedings of the Royal Society, Biology Letters* **1**, 176–7.

Chiappe, L.M. 1991 Cretaceous birds of Latin America. *Cretaceous Research* **12**, 55–63.

Chiappe, L.M. 1992 Enantiornithine tarsometatarsi and the avian affinities of the late Cretaceous Avisauridae. *Journal of Vertebrate Paleontology* **12**, 344–50.

Chiappe, L.M. 1993 Enantiornithine (Aves) tarsometatarsi from the Cretaceous Lecho Formation of northwestern Argentina. *American Museum Novitates* **3083**, 1–27.

Chiappe, L.M. 1996 Early avian evolution in the southern hemisphere: fossil record of birds in the Mesozoic of Gondwana. *Memoirs of the Queensland Museum* **39**, 533–56.

Chiappe, L.M. 2002 Basal bird phylogeny: problems and solutions. In L.M. Chiappe and L.M. Witmer (eds), *Mesozoic birds: above the heads of dinosaurs*, 448–72. Berkeley. University of California Press.

Chiappe, L.M. 2007 *Glorified dinosaurs: the origin and early evolution of birds*. London. John Wiley and Sons.

Chiappe, L.M. and Calvo, J.O. 1994 *Neuquenornis volans*, a new Enantiornithes (Aves) from the Upper Cretaceous of Patagonia. *Journal of Vertebrate Paleontology* **14**, 230–46.

Chiappe, L.M. and Dyke, G.J. 2002 The Cretaceous radiation of birds. *Annual Reviews of Ecology and Systematics* **33**, 91–124.

Chiappe, L.M. and Witmer, L.M. 2002 Mesozoic birds: above the heads of dinosaurs. Berkeley. University of California Press.

Chiappe, L.M. and Walker, C.A. 2002 Skeletal morphology and systematics of the Cretaceous euenantiornithes (Ornithothoraces: Enantiornithes). In L.M. Chiappe and L.M. Witmer (eds), *Mesozoic birds: above the heads of dinosaurs*, 240–67. Berkeley. University of California Press.

Chiappe, L.M., Suzuki, S., Dyke, G.J., Watabe, M., Tsogtbaatar, M. and Barsbold, R. 2007 A new enantiornithine bird from the Late Cretaceous of the Gobi Desert. *Journal of Systematic Palaeontology* **5**, 193–208.

Christiansen, P. and Bonde, N. 2000 Axial and appendicular pneumaticity in *Archaeopteryx*. *Proceedings of the Royal Society of London, Series B (Biological Sciences)* **267**, 2501–05.

Cornell Lab of Ornithology 2004 *Cornell lab of ornithology: handbook of bird biology*. Princeton. Princeton University Press.

Dyke, G.J. and Ösi, A. 2010 A review of Late Cretaceous fossil birds from Hungary. *Geological Journal* **45(4)**, 434–44 (Online April 2010: 10.1002/gj.1209).

Elzanowski, A. 1981 Embryonic bird skeletons from the late Cretaceous of Mongolia. *Palaeontologica Polonica* **42**, 147–76.

Feduccia, A. 1999 *The origin and evolution of birds*, 2nd edn. New Haven. Yale University Press.

Feduccia, A. 2006 Mesozoic aviary takes form. *Proceedings of the National Academy of Sciences* **103**, 5–6.

Fountaine, T.M.R., Benton, M.J., Dyke, G.J. and Nudds R.L. 2005 The quality of the fossil record of Mesozoic birds. *Proceedings of the Royal Society of London, Series B (Biological Sciences)* **272**, 289–94.

Harrison, C.J.O. and Walker, C.A. 1973 *Wyleyia*: a new bird humerus from the lower Cretaceous of England. *Palaeontology* **16**, 721–8.

Howard, H. 1929 The avifauna of Emeryville Shellmound. *University of California*, *Publications in Zoology* **32**, 78–88.

Kurochkin, E.N. 1995 Synopsis of Mesozoic birds and early evolution of class Aves. *Archaeopteryx* **13**, 47–66.

Kurochkin, E.N. 1999 A new large enantiornithid from the Late Cretaceous of Mongolia (Aves, Enantiornithes). *Trudy Zoologicheskogo Instituta RAN* **277**, 130–41.

Linnaeus, C. 1758 *Systema naturae per regna tria naturae*, 10th edn. Holmiae. L. Salmi.

Martin, L.M. 1983 The origin and early radiation of birds. In A.H. Brush and G.A. Clark, Jr (eds), *Perspectives in ornithology*, 291–338. Cambridge. Cambridge University Press.

Mayr, G., Pohl, B. and Peters, D.S. 2005 A well-preserved *Archaeopteryx* specimen with theropod features. *Science* **310**, 1483–6.

Mayr, G., Pohl, B., Hartman, S. and Peters, D.S. 2006 The tenth skeletal specimen of *Archaeopteryx*. *Zoological Journal of the Linnean Society* **149**, 97–116.

Nessov, L.A. 1984 Pterosaurs and birds of the late Cretaceous of Central Asia. *Paleontological Journal* **1**, 47–57 [in Russian].

Ösi, A. 2008 Enantiornithine bird remains from the Late Cretaceous of Hungary. *Oryctos* **7**, 55–60.

O'Connor, P.M. 2004 Pulmonary pneumaticity in the postcranial skeleton of extant Aves: a case study examining Anseriformes. *Journal of Morphology* **261**, 141–61.

O'Connor, P.M. and Claessens, L.P.A.M. 2005 Basic avian pulmonary design and flow-through ventilation in theropod dinosaurs. *Nature* **436**, 253–6.

Sanz, J.L., Chiappe, L.M. and Buscalioni, A.D. 1995 The osteology of *Concornis lacustris* (Aves: Enantiornithes) from the Lower Cretaceous of Spain, and a reexamination of its phylogenetic relationships. *American Museum Novitates* **3133**, 1–23.

Walker, C.A. 1981 New subclass of birds from the Cretaceous of South America. *Nature* **292**, 51–3.

Walker, C.A. n.d. Cretaceous birds of Argentina. Unpublished manuscript and photographs.

Walker, C.A., Buffetaut, E. and Dyke, G.J. 2007 Large euenantiornithine birds from the Cretaceous of southern France, North America and Argentina. *Geological Magazine* **144**, 977–86.

Zhang, F. and Zhou, Z. 2000 A primitive enantiornithine bird and the origin of feathers. *Science* **290**, 1955–9.

Zhang, F., Zhou, Z., Hou, L. and Gu, G. 2000 Early diversification of birds—evidence from a new opposite bird. *Chinese Science Bulletin* **45**, 2650–7.

CYRIL A. WALKER†
c/o Department of Palaeontology,
The Natural History Museum, London,
Cromwell Road,
London,
SW7 5BD,
UK.

†While this paper was in its final stages (May 2009), Cyril Walker passed away. He had been working on variants of this manuscript for many years; Gareth Dyke contributed by helping him to complete the writing and to steer this paper through the journal process.

GARETH J. DYKE (corresponding author)
School of Biology and Environmental Science,
University College Dublin,
Belfield,
Dublin 4,
Ireland.

E-mail: gareth.dyke@ucd.ie

Table 1—Fossil Euenantiornithine bird specimens collected from the Argentine locality of El Brete in the 1970s.

Specimen number	*Elements*	*Original reference*	*Subsequent reference*	*Original taxonomic placement*	*Current taxonomic placement*
PVL 4035 (holotype)	Proximal left scapula; left coracoid; proximal left humerus	Walker (1981)	Chiappe (1996); Chiappe and Walker (2002)	*Enantiornis leali* Walker (1981)	*Enantiornis leali* (Walker 1981)
PVL 4020	Left scapula; imperfect left coracoid; left humerus; broken left ulna; proximal right ulna-radius; right scapholunar; right cuneiform; proximal right carpometacarpus with pollex (pollex lost)	Walker (n.d.)[1]	Chiappe (1996) Chiappe and Walker (2002)	*Enantiornis leali* (Chiappe 1996)	*Enantiornis leali* (Chiappe 1996)
PVL 4039 PVL 4055	Two complete scapulae	Walker (n.d.)	Chiappe (1996) Chiappe and Walker (2002)	*Enantiornis leali* (this paper)	*Enantiornis leali* (Chiappe 1996)
PVL 4029	Imperfect right coracoid	Walker (n.d.)		*Enantiornis leali* (this paper)	*Enantiornis leali* (this paper)
PVL 4023	Proximal ulna	Walker (n.d.)	Chiappe (1996) Chiappe and Walker (2002)	*Enantiornis leali* (Chiappe 1996)	*Enantiornis leali* (Chiappe 1996)
PVL 4050 PVL 4057	Two cervical vertebrae	Walker (n.d.)	Chiappe and Walker (2002)	*Enantiornis* sp. (Walker n.d.)	Enantiornithes uncertain (this paper)
PVL 4021[2]	Imperfect sternum with marked keeled carina	Walker (n.d.)	Chiappe (1991, 1992)	*Enantiornis* sp. (Walker n.d.)	*Enantiornis leali* (this paper)
PVL 4045	Sacrum	Walker (n.d.)	Chiappe and Walker (2002)	*Enantiornis* sp. (Walker n.d.)	*Enantiornis* sp. (this paper)
PVL 4042	Associated ilium and ischium (right side)	Walker (n.d.)		*Enantiornis* sp. (Walker n.d.)	*Enantiornis* sp. (this paper)
PVL 4043	Proximal left humerus	Walker (n.d.)	Chiappe and Walker (2002)	*Enantiornis* sp. (Walker n.d.)	*Enantiornis leali* (this paper)
PVL 4021 (holotype)*	Left tibiotarsus and tarsometatarsus	Walker (n.d.)	Chiappe (1993) Chiappe and Walker (2002)	*Enantiornis* sp. (Walker n.d.)	*Lectavis bretincola* (Chiappe 1993)

Table 1 (*cont.*)—Fossil Euenantiornithine bird specimens collected from the Argentine locality of El Brete in the 1970s.

Specimen number	*Elements*	*Original reference*	*Subsequent reference*	*Original taxonomic placement*	*Current taxonomic placement*
PVL 4040	Tarsometatarsus	Walker (n.d.)	Chiappe (1993)	*Enantiornis* sp. (Walker n.d.)	*Yungavolucris brevipedalis* (Chiappe 1993)
PVL 4052	Tarsometatarsus	Walker (n.d.)	Chiappe (1991)	*Enantiornis* sp. (Walker n.d.)	*Yungavolucris brevipedalis* (Chiappe 1993)
PVL 4053 (holotype)	Right tarsometatarsus	Walker (n.d.)	Chiappe (1991, 1992, 1993)	*Enantiornis* sp. (Walker n.d.)	*Yungavolucris brevipedalis* (Chiappe 1993)
PVL 4268	Tarsometatarsus	Walker (n.d.)	Chiappe (1993)	*Enantiornis* sp. (Walker n.d.)	*Yungavolucris brevipedalis* (Chiappe 1993)
PVL 4058	Metatarsal bone (III and IV trochlea)	Walker (n.d.)		*Enantiornis* sp. (Walker n.d.)	*Enantiornis* sp. (this paper)
PVL 4054 (holotype)	Left humerus	Walker (n.d.)	Chiappe and Walker (2002) Walker *et al*. (2007)	*Martinavis vincei* (Walker *et al*. 2007)	*Martinavis vincei* (Walker *et al*. 2007)
PVL 4059 (paratype)	Distal end of left humerus	Walker (n.d.)	Walker *et al*. (2007)	*Martinavis vincei* (Walker *et al*. 2007)	*Martinavis vincei* (Walker *et al*. 2007)
PVL 4025 (holotype)	Almost complete left humerus	Walker (n.d.)	Chiappe and Walker (2002) Walker *et al*. (2007)	*Martinavis* sp. (Walker *et al.* 2007)	*Martinavis saltariensis* (this paper)
PVL 4046 (holotype)	Proximal left humerus	Walker (n.d.)	Walker *et al*. (2007)	*Martinavis* sp. (Walker *et al*. 2007)	*Martinavis minor* (this paper)
PVL 4028 (holotype)	Proximal left humerus	Walker (n.d.)	Walker *et al*. (2007)	*Martinavis* sp. (Walker *et al*. 2007)	*Martinavis whetstonei* (this paper)
PVL 4034 (a)[3]	Imperfect right scapula	Walker (n.d.)	Chiappe and Walker (2002)	cf. *Martinavis* (Walker n.d.)	cf. *Martinavis* (this paper)
PVL 4034 (b)[3]	Right coracoid (?associated with above)	Walker (n.d.)	Chiappe and Walker (2002)	cf. *Martinavis* (Walker n.d.)	cf. *Martinavis* (this paper)
PVL 4031	Complete left ulna	Walker (n.d.)		cf. *Martinavis* (Walker n.d.)	cf. *Martinavis* (this paper)
PVL 4044	Proximal end of right ulna	Walker (n.d.)		cf. *Martinavis* (Walker n.d.)	cf. *Martinavis* (this paper)

Table 1 (*cont.*)—Fossil Euenantiornithine bird specimens collected from the Argentine locality of El Brete in the 1970s.

Specimen number	*Elements*	*Original reference*	*Subsequent reference*	*Original taxonomic placement*	*Current taxonomic placement*
PVL 4056	Complete right radius	Walker (n.d.)		cf. *Martinavis* (Walker n.d.)	cf. *Martinavis* (this paper)
PVL 4049	Distally imperfect carpometacarpus	Walker (n.d.)	Chiappe and Walker (2002)	cf. *Martinavis* (Walker n.d.)	*Enantiornis leali* (Chiappe and Walker 2002) *Martinavis* sp. (this paper)[4]
PVL 4037	Complete right femur	Walker (n.d.)	Chiappe and Walker (2002)	cf. *Martinavis* (Walker n.d.) Chiappe and Walker (2002) euenantiornithine	*Martinavis* sp.? (Walker *et al.* 2007; this paper)
PVL 4038	Complete right femur	Walker (n.d.)	Chiappe and Walker (2002)	cf. *Martinavis* (Walker n.d.)	*Martinavis* sp. nov. (this paper)
PVL 4060	Complete left femur	Walker (n.d.)	Chiappe and Walker (2002)	cf. *Martinavis* (Walker n.d.)	*Martinavis* sp. nov. (this paper)
PVL 4033	Complete right tibiotarsus	Walker (n.d.)	Chiappe and Walker (2002)	cf. *Martinavis* (Walker n.d.)	*Soroavisaurus australis* (Chiappe and Walker 2002)
PVL 4032	Proximal end of left tibiotarsus; distal end of right ulna	Walker (n.d.)	Chiappe and Walker (2002)[5]	cf. *Martinavis* (Walker n.d.)	*Martinavis* sp. (this paper)
PVL 4036	Right femur	Walker (n.d.)		cf. *Martinavis* (Walker n.d.)	cf. *Martinavis* (this paper)
PVL 4030	Distal end of right tibiotarsus	Walker (n.d.)	Chiappe and Walker (2002)	cf. *Martinavis* (Walker n.d.)	*Martinavis* sp. nov. (this paper)
PVL 4022 (holotype)	Right scapula; right coracoid; left humerus; right radius, ulna	Walker (n.d.)	Chiappe and Walker (2002)	*Elbretornis bonapartei* (Walker n.d.)	*Elbretornis bonapartei* gen. et sp. nov. (this paper)
PVL 4047 PVL 4051	Thoracic vertebrae	Walker (n.d.)	Chiappe and Walker (2002)	*Elbretornis* sp.? (Walker n.d.)	Chiappe and Walker (2002)[6] euenantiornithine
PVL 4041	Imperfect synsacrum; distal half of right femur; rib fragments	Walker (n.d.)	Chiappe and Walker (2002) euenantiornithine	*Elbretornis* sp.? (Walker n.d.)	*Elbretornis* sp.? (Walker n.d.)
PVL 4027	Imperfect right tibiotarsus	Walker (n.d.)		*Elbretornis* sp.? (Walker n.d.)	*Elbretornis* sp. (this paper)

Table 1 (*cont.*)—Fossil Euenantiornithine bird specimens collected from the Argentine locality of El Brete in the 1970s.

Specimen number	*Elements*	*Original reference*	*Original reference*	*Subsequent reference*	*Current taxonomic placement*
PVL 4048 (holotype)	Complete left tarsometatarsus, phalanges and claws	Walker (n.d.)	Chiappe (1991, 1992) Brett-Surman and Paul (1985) Chiappe 1992; Chiappe and Calvo 1994	Gen. et sp. indet. (Walker n.d.) *Avisaurus* Brett-Surman and Paul (1985)	*Soroavisaurus australis* (Chiappe 1993)
PVL 4690 (holotype)	Tarsometatarsus	Walker (n.d.)	Chiappe (1992)	Chiappe (1992) *Avisaurus* sp.	*Soroavisaurus australis* (Chiappe 1993)
PVL 4692	Incomplete tarsometatarsus, trochlea of mt II and III	Walker (n.d.)	Chiappe (1993)		*Yungavolucris brevipedalis* (Chiappe 1993)
PVL 4181	Isolated ulna	Walker (n.d.)	Chiappe (1996)	*Enantiornis leali* (Chiappe 1996)	*Enantiornis leali* (Chiappe 1996)
PVL 4698	Right mandibular ramus (dentary)	Walker (n.d.)	Chiappe and Walker (2002)	Walker (n.d.) enantiornithine?	Chiappe and Walker (2002) Tentatively euenantiornithine
PVL 4273	Femur	Chiappe and Walker (2002)		Chiappe and Walker (2002) euenantiornithine	cf. *Martinavis* this paper
PVL 4265	Proximal right humerus and shaft				Euenantiornithine this paper
PVL 4267	Ulna				*Enantiornis leali* this paper
PVL 4266	Proximal end of right humerus				*Enantiornis leali* this paper
PVL 4180	Proximal left humerus				Enantiornithine this paper
PVL 4271	Complete coracoid				*Enantiornis leali* this paper
PVL 4272	Partial coracoid				cf. *Enantiornis* this paper

(Endnotes)

1 References to Walker (n.d.) denote an unpublished but completed paper dealing with this El Brete collection reposited in the BMNH by CAW in the mid-1980s.

2 Walker (n.d.) noted that the association between this sternum and leg elements bearing the same number was doubtful (J. Bonaparte, pers. comm. 1980). At least one of these specimens will require a new PVL number. Similarly, it is likely that *Lectavis* (Chiappe 1993) is a junior synonym of *Enantiornis* (given specimen associations and the hindlimb measurements of Enantiornis; Walker 1981, n.d.).

3 We have inserted (a) and (b) to allow us to distinguish these two elements in our discussions; their association is certain (Walker n.d.).

4 Our reassessment shows that PVL 4049 is too small (width of proximal articulation, 4mm) to correspond with elements already referred to the much larger *Enantiornis leali* (Walker 1981; Chiappe 1996; Chiappe and Walker 2002).

5 Pelvis PVL 4042 was figured by Chiappe and Walker (2002) using the number PVL 4032.

6 Chiappe and Walker (2002: 248) noted that additional thoracic vertebrae have been collected from El Brete 'more recently'. This material has not yet been described.

Table 2—Selected measurements (in mm) of elements referred to Euenantiornithine birds.

Enaliornis leali				
	Holotype			
Humerus:	*4035*		*4043*	*4020*
Maximum width, bicipital to deltopectoral crest	26.9		27.8	25.2
Craniocaudal depth of head	7		7.5	6.6
Craniocaudal depth of external tub.	7.7		8.2	6.5
Craniocaudal depth from internal tub.	17.3		16.5	14.6
Length of bicipital crest	12.1		14.5	13.5
Width of capital groove			3.5	3.3
Width of pneumatic foramen	4.1		3.5	3.8
Total length (est.)				141.2
Scapula:	*4035*	*4039*	*4055*	*4020*
Maximum length		89	78.5	75.4
Anteroposterior length	23.2	23.1	21.2	21.5
Anteroposterior length of glenoid facet	12.7	12.8	12.5	12.2
Lateromedial depth of glenoid facet	9.4	9.5	9.4	9.3
Lateromedial depth of coracoidal facet	9.4	9.5	9.3	9.2
Width of neck between coracoidal facet and furcular articulation	8.9	9.5	9.3	7.2
Lateromedial length of articular surface at furcular articulation	13.4	14.1	13.1	12.4
Anteroposterior width of notch anterior to coracoid articulation	2.6	2	2.8	2.8
Coracoid:	*4035*	*4029*		*4020*
Maximum length	77.2			66.4
Anteroposterior length of articular surface	7.9			7
Length of scapular articulation	6.2			5
Lateromedial width of scapular articulation	6.4			6.8
Width of glenoid facet	12.2			10.1
Length of shaft from distal margin to dorsal foramen	4.6			4.8
Lateromedial width of sternal end	18.6	15.7		

Enaliornis leali			
Ulna:	*4023*		*4020*
Maximum length			146
Maximum lateromedial width across cotylae	19		16.8

Table 2 (*cont.*)—Selected measurements (in mm) of elements referred to Euenantiornithine birds.

Craniocaudal depth from internal cotyla	12	11.7
Craniocaudal depth from external cotyla	5.5	5.4
Width from olecranon to external cotyla	13.1	11.9
Maximum distal medial width		11.7
Maximum distal lateral width		12.8
Width of shaft in medial view	11	8.7
Radius:		
Maximum length		142.1
Carpometacarpus:		
Maximum anterior width of carpal trochlea		8.4
Length of metacarpal II		7.3
Length from metacarpal II to carpal trochlea		13.6

Enantiornis sp.

Ilium and ischium:	*4042*
Maximum length of ilium	64
Length of anterior blade from anterior rim of acetabulum	31.5
Length of posterior projection of ilium	25.1
External depth of acetabulum	7.2
Internal depth of acetabulum	7
Length of ilioishiadic fenestra	15.4
Depth of ilioishiadic fenestra	8.9
Length of antitrochanter	6.1

Martinavis vincei

	Holotype	
Humerus:	*4054*	*4059*
Maximum length	110	
Proximal width bicipital to deltopectoral crest	22.2	
Craniocaudal depth between crests	4.6	
Craniocaudal depth at external tuberosity	5.9	
Craniocaudal depth at internal tuberosity	14	
Length of deltopectoral crest	25.4	

Table 2 (*cont.*)—Selected measurements (in mm) of elements referred to Euenantiornithine birds.

Medial length of bicipital crest	10	
Width of capital groove	3.9	
Width of pneumatic fossa	9.7	
Craniocaudal width of head	7.6	
Maximum width of distal end	20	20
Ectepicondyle prominence to ectepicondyle	9.2	9.2
Craniocaudal width of external condyle	7.9	7
Proximodistal width of external condyle	3.3	3.3
Proximodistal width of olecranon fossa	7.9	7.9

Martinavis sp.

Humerus:	*KU-NM 37*
Lateromedial width from external tuberosity to bicipital crest	29.5
Craniocaudal depth of head at depression	7.8
Craniocaudal depth of external tuberosity	6.9
Craniocaudal depth of internal tuberosity	13.8
Medial length of bicipital crest	16.6
Width of capital groove	6.8
Maximum width of pneumatic fossa	17.7
Craniocaudal width of head	14

Martinavis sp.

Radius:	*4056*
Maximum length	117.8
Maximum proximal width	7.6
Maximum distal width	8.7
Carpometacarpus:	*4049*
Width of proximal articulation	4
Maximum width of proximal articulation	6.6
Scapula:	*4034*
Maximum length	62
Anteroposterior length from furcular articulation to glenoid	17.7
Anteroposterior length of glenoid	10

Table 2 (*cont.*)—Selected measurements (in mm) of elements referred to Euenantiornithine birds.

Lateromedial depth of glenoid	5.8			
Lateromedial depth of coracoid facet	5.5			
Minimal lateromedial width of neck between coracoidal facet	5.6			
Length of articulation surface at coracoidal articulation	7.1			
Coracoid:	*4034*			
Maximum length	50			
Anteroposterior length of proximal articulation	14.8			
Length of scapular facet	5			
Lateromedial width of scapular facet	4.8			
Width of glenoid facet	4.9			
Length of shaft from distal margin to coracoid foramen	10.2			
Lateromedial width of sternal end	15.1			
Martinavis sp.				
Ulna:	*4044*	*4032*	*4031*	
Maximum length			70.8	
Maximum lateromedial width across internal-external cotyla	10.9	10	7.2	
Craniocaudal depth from rim of internal cotyla	7.7		6	
Craniocaudal depth of external cotyla	3.6			
Width from olecranon to external cotyla	10.7		7.2	
Maximum palmar distal width		9.6		
Maximum width of shaft above distal articulation		6.5	4.7	
Femur:	*4037*	*4038*	*4036*	*4060*
Maximum length	77.8	75.6	55	
Width from head to lesser trochanter	16	14.2	11.2	10.5
Greater trochanter to head	11.2	10.1	9.5	9.3
Anteroposterior width of head	6.2	5.9	4	4.2
Anteroposterior width of greater trochanter proximally	8.5	8.5	5.5	6.7
Lesser trochanter-internal condyle	73.3	69.2	51.2	
Maximum lateromedial width of distal end	11.8	11	8.7	
Lateromedial width of internal condyle	5.1	4.8	3.4	
Lateromedial width of external condyle	5.7	5.6	3.5	
Antero-posterior width of internal condyle	8.1	7.9	5.5	
Antero-posterior width of external condyle	9.5	8.4	5.9	

Table 2 (*cont.*)—Selected measurements (in mm) of elements referred to Euenantiornithine birds

Martinavis sp.			
Tibiotarsus:	*4032*	*4033*	*4030*
Maximum length		85.6	
Maximum latero-posterior width of proximal end	11	10.2	
Maximum antero-posterior width	10.7	10.7	
Lateromedial width of shaft below proximal articulation	7.8	7.1	
Maximum lateromedial width of internal-external condyles (anterior)		11.7	7.8
Maximum lateromedial width of internal-external condyles (posterior)		9.1	7.5
Antero-posterior depth of internal condyle		9.1	6.1
Antero-posterior depth of external condyle		8	6.5
Proximodistal depth of internal condyle		7.5	6
Proximodistal depth of external condyle		6.5	5.5
Midline medial width of internal condyle		6.7	2.5
Midline medial width of external condyle		6.4	4.9
Maximum antero-posterior depth of condyles		9.2	6.5

Martinavis saltariensis	
	Holotype
Humerus:	*4025*
Maximum length	95.3
Length from bicipital crest to deltoid crest	20.9
Craniocaudal depth at depression	5.3
Craniocaudal depth at external tuberosity	6.2
Craniocaudal depth at internal tuberosity	9.4
Length of deltopectoral crest	25.4
Width of capital groove	
Medial length of bicipital crest	9.7
Maximum width of pneumatic fossa	8
Width of head craniocaudally	6.7
Maximum lateromedial width of distal end	20.8
Ectepicondylar prominence—ectepicondyle	6.3
Medial margin of external condyle—ectepicondyle	9.2
Craniocaudal width of external condyle	5.5
Craniocaudal width of internal condyle	6.2

Table 2 (*cont.*)—Selected measurements (in mm) of elements referred to Euenantiornithine birds

Martinavis minor	
	Holotype
Humerus:	*4046*
Length from bicipital crest to deltoid crest	14.8
Craniocaudal depth at depression	3.1
Craniocaudal depth at external tuberosity	3.3
Craniocaudal depth at internal tuberosity	7.4
Length of deltopectoral crest	7.1
Medial length of bicipital crest	6.7
Width of capital groove	2
Maximum width of pneumatic fossa	4
Width of head craniocaudally	4.2

Martinavis whetstonei	
	Holotype
Humerus:	*4028*
Maximum width external tuberosity to bicipital crest	15.4
Craniocaudal depth at depression	2.5
Craniocaudal depth at external tuberosity	4.2
Craniocaudal depth at internal tuberosity	6.1
Length of deltopectoral crest	6.3
Medial length of bicipital crest	7
Maximum width of pneumatic fossa	1.6

Elbretornis bonapartei	
	Holotype
Humerus:	*4022*
Maximum length	90.2
Length from bicipital crest to deltoid crest	20.4
Craniocaudal depth at depression	4
Craniocaudal depth at external tuberosity	5.4
Craniocaudal depth at internal tuberosity	13.1
Length of deltopectoral crest	23.5
Medial length of bicipital crest	9.8

Table 2 (*cont.*)—Selected measurements (in mm) of elements referred to Euenantiornithine birds

Width of capital groove	1.8
Maximum width of pneumatic fossa	5.7
Width of head craniocaudally	6.4
Medial margin of external condyle—ectepicondyle	9
Ectepicondylar prominence—ectepicondyle	6.4
Coracoid:	*4022*
Maximum width of sternal end	12
Ulna:	*4022*
Maximum lateromedial width of proximal end	10.9
Olecranon-external condyle	11.5
Elbretornis sp.	
Femur:	*4041*
Maximum lateromedial width at distal articulation	8.5
Lateromedial width of internal condyle (posterior)	3.8
Lateromedial width of external condyle (posterior)	2.5
Antero-posterior width of internal condyle	7.2
Antero-poterior width of external condyle	8.2
Tibiotarsus:	*4027*
Maximum length	78.5
Maximum lateromedial width at proximal articulation	8.3
Maximum lateromedial width at distal articulation	7.8
Synsacrum:	*4041*
Antero-posterior length of ilium	41
Depth of ilium above acetabulum	8.6
Acetabulum to anterior margin of ilium	19.6